Influence of flow containment and substrate entrainment upon sandy hybrid event beds containing a co-genetic mud-clast-rich division

S. J. Southern [a1] *, M. Patacci [a2], F. Felletti [b3], W. D. McCaffrey [a4]

[a] Turbidites Research Group, School of Earth & Environment, University of Leeds, Leeds, LS2 9JT, United Kingdom

[b] Dipartimento di Scienze della Terra, Università degli Studi di Milano, Via Mangiagalli 34, 20034 5 Milano, Italy

Abstract

Individual sandstone beds containing a co-genetic mud-clast-rich (MCR) division are being increasingly described from the distal reaches of many deep-water fan systems. These deposits, termed hybrid event beds, are considered to record a flow whose composition and rheology changed significantly to become increasingly more argillaceous (clay-rich), MCR and turbulence-suppressed during the deposition of a single event bed. Studies of confined systems, in which gravity flows were affected by confining sea-floor topography, have documented similar deposits recording turbulence suppression in proximity to confining sea-floor topography (e.g., basin margins). In new research from a confined, contained system from the Castagnola Basin of NW Italy, lateral transects of individual sandstone beds 5 km in extent show that individual sandstones beds contain a co-genetic MCR division which is often; 1) extensive across the basin rather than localised adjacent to confining topography; 2) exhibits rapid, significant and repeated variation in depositional character over short length scales (tens to hundreds of metres), specifically in terms of the thickness of co-genetic MCR

[1] *Corresponding author: ee06s2s@leeds.ac.uk, +447795690988.
[2] m.patacci@leeds.ac.uk
[3] fabrizio.felletti@unimi.it
[4] w.d.mccaffrey@leeds.ac.uk

divisions and the size and abundance of clasts contained within them; and 3) exhibits variation in depositional character over larger length scales (>1 km) which is non-systematic in relation to palaeoflow direction or increasing proximity towards the counter slope of the downstream confining northern basin margin. A suite of factors within the Castagnola Basin is thought to have resulted in the deposition of these co-genetic MCR divisions whose thickness and distribution are less predictable in relation to confining sea-floor topography than those described from other confined uncontained settings. Specific factors include; 1) recent and voluminous entrainment of muddy substrate at seemingly random locations across the basin floor and their support and transport within a high sediment concentration gravity flow; and 2) containment (ponding) of gravity flows within a confined basin, which is thought to have established extensive and complex three dimensional flow dynamics across the basin following flow interaction with multiple basin margins. This research highlights the role of entrainment of muddy substrate and subsequent transport processes of muddy substrate for developing co-genetic MCR divisions, as well as the importance of understanding the degree of containment depositional systems experienced when considering the spatial distribution of depositional facies, and thus reservoir quality, in topographically complex settings.

Key words: hybrid event bed; ponded flow; mud-clast-rich deposits; onlap facies; turbidite; flow confinement

1. Introduction

Hybrid event beds (HEB) are now recognised as a significant component of deep-water systems from a variety of settings (e.g., Haughton et al., 2003, 2009; Talling et al., 2004, 2012a; Amy and Talling, 2006; Davis et al., 2009; Hodgson, 2009; Muzzi Magalhaes and Tinterri, 2010; Patacci et al., 2014). Frequently these deposits comprise a mud-clast-rich (MCR) argillaceous (clay-rich) sandstone which directly overlies unstratified to stratified relatively cleaner (clay-poor) sandstones; both facies are co-genetic, having been emplaced during a single gravity-driven current event (Haughton et al., 2003, 2009; Talling et al., 2004; Talling, 2013). HEBs are considered to reflect deposition beneath a passing flow event which evolved significantly in terms of composition and rheology (e.g., becoming increasingly argillaceous, MCR and turbulence- suppressed (Haughton et al., 2009)). Such flow evolution has been attributed to distal or lateral flow transformations, following significant entrainment of a muddy substrate, and or declining turbulence energy (e.g., Ricci Lucchi and Valmori, 1980; Haughton et al., 2003, 2009; Amy and Talling, 2006; Barker et al., 2008; Hodgson, 2009; Muzzi Magalhaes and Tinterri, 2010; Patacci et al., 2014). HEBs are of great significance as they are characterised by marked heterogeneity in depositional character, and thus reservoir quality, on an intra-bed scale (e.g., Sylvester and Lowe, 2004) and can be an indicator of cleaner, better reservoir quality sandstone farther upstream (e.g., Haughton et al., 2003; Hodgson, 2009).

Typically HEBs have been described from the distal parts of unconfined systems with relatively subdued sea-floor topography (e.g., Haughton et al., 2003, Amy and Talling, 2006; Hodgson, 2009); however HEBs and other deposits interpreted to record increasingly argillaceous, MCR and turbulence suppressed deposition during a single flow event have been recognized in more topographically complex settings (e.g., Barker et al., 2008; Patacci et al., 2014). In such settings sea-floor topography can modify gravity current transport direction, velocity and deposition (e.g., Kneller et al., 1991; Kneller and McCaffrey, 1999; Jackson and Johnson, 2009; Athmer and Luthi, 2011; Gamberi and Rovere, 2011); herein termed flow confinement. Additionally the term flow containment can be applied where sea-floor topography encircles and retains a flow within a depositional low (e.g., a ponded mini-basin), and the size or thickness of the flow is sufficient such that it feels the effects of this containment (Van Andel and Komar, 1969; Pantin and Leeder, 1987). Thus depositional systems in this study are classified as either unconfined and uncontained (UU), confined and uncontained (CU), or confined and contained (CC; Fig. 1). Contained systems are always associated with flow confinement processes due to the presence of encircling confining sea-floor topography in such settings. From a CU setting Barker et al. (2008) document the increasing thickness of argillaceous sandstone at the expense of underlying co-genetic relatively clean sandstone within the same bed towards a laterally confining basin margin; they interpret such a depositional trend to record increasing turbulence suppression due to flow thinning with distance towards the lateral basin margin. Lateral variation in the depositional character of individual beds towards their onlap onto a confining basin margin has also been documented in the outcrop from a CU system (Annot Sandstone, SE France; Patacci et al. 2014). Patacci et al. (2014) describe the systematic development and thickening of a co-genetic MCR division, and the development of a HEB, at the expense of mud-clast-poorer, cleaner sandstone within the same bed locally (<1 km) towards the confining basin margin. They interpreted such a depositional trend to result from the localized confining effects of the basin margin. Observations from such studies suggest that forced flow transformation adjacent to confining topography can result in development of a predictable deposit character and depositional trends towards such topography; such onlapping deposits are of great importance where they form stratigraphic traps in hydrocarbon reservoirs. This study presents examples of HEB depositional character and distribution within a CC setting and demonstrates that their distribution may not be predictable where flow containment occurs in addition to flow confinement. Our observations highlight the role of muddy substrate entrainment and the combined effects of flow confinement and containment upon gravity flow dynamics and deposit character, and thus reservoir quality distribution, and how these might vary in topographically complex settings with differing degrees of flow containment.

2. Geological Setting

The Tertiary Piedmont Basin of NW Italy was an episutural basin formed during late Cretaceous to late Eocene Meso-Alpine collision of the European plate and Adria micro-plate (Ricci Lucchi, 1986; Biella et al., 1992; Maino et al., 2013) (Fig. 2a-c). The eastern Tertiary Piedmont Basin contains a late Eocene to early Miocene deep-water turbiditic succession (c. 3000 m thick, Fig. 2a) with several major unconformities, most common earlier in the succession, recording regional tectonic events that caused important changes in basin physiography (Cavanna et al., 1989; Di Giulio and Galbiati, 1993). Transpressive motion along the E-W trending Villalvernia-Varzi line in the easternmost Tertiary Piedmont Basin during the Chattian-Aquitanian folded Oligocene strata to form the asymmetric, ENE-WSE trending Castagnola sub-basin (Ibbeken, 1978; Andreoni et al., 1981; Cavanna et al., 1989; Di Giulio and Galbiati, 1993) (Fig. 2b, c)

Sediment gravity currents entered the Castagnola Basin from the SW (Stocchi et al., 1992) and emplaced the c. 800 m thick Castagnola Formation which onlapped the underlying Rigoroso Formation (Cavanna et al., 1989; Andreoni et al., 1981; Di Giulio and Galbiati, 1993) (Fig. 2a-c). During emplacement of the Costa Grande Member, termination of activity on the Villalvernia-Varzi line around the Chattian-Aquitanian boundary forced a change from deposition of laterally offset, stacked sand bodies, to simple sheet-like deposits (e.g., sub-units A-H and sub-unit I, respectively, of Felletti, 2002, 2004b); the latter style of deposition persisted throughout the remainder of the Costa Grande Member (Stocchi et al., 1992; Baruffini et al., 1994). Outcrop upstream (south) of the basin is sparse, and thus little is known of the shelf and feeder system to the Castagnola Basin. Estimates of the basin width (c. 11 km) and basin length downstream (c. 5 km) are constrained by the extent of Costa Grande Member deposits. However, this basin area would have necessarily increased during progressive infill of a basin with inclined (i.e., non-vertical) basin margin slopes. Gravity currents emplacing the Costa Grande member were contained (ponded) within the basin, resulting in the development of thick mud caps between beds (Stocchi et al., 1992; Baruffini et al., 1994), palaeocurrent indicators of flow reflection and deflection at the downstream counter slope of the northern basin margin, and a lack of comparable correlative strata beyond the basin (Stocchi et al., 1992; Felletti, 2002)(Fig. 2c). Dips on the northern basin margin at the time of deposition are estimated to be on the order of 10° (Baruffini et al., 1994; Felletti, 2002, 2004a).

3. Methods

A well exposed interval (c. 250 m stratigraphic thickness) within the turbiditic Costa Grande Member was logged using a Jacob staff at eight separate locations across the Castagnola sub-basin (Figs. 1d, 2c). Together these logs form a 4.9 km-long transect orientated slightly oblique (030/045-210/225°) to the palaeoflow direction of gravity currents entering the basin (SW-NE), and highly oblique to the E-W striking confining northern basin margin and palaeoflow direction of deflected gravity currents here (~W-E). High-confidence correlation of individual beds was aided by good exposure, the presence of several distinct thick marker beds, and the tabular nature of the interval at this level within the Costa Grande Member (Fig. 2d). These correlations confirm those of Stocchi et al. (1992) and Felletti (2002) and provided the framework for assessing bed characteristics spatially (palaeogeographically and stratigraphically) in relation to the confining counter-slope at the northern basin margin. Where outcrop permitted, transects of key beds were made at specific locations, over distances of up to 100 m, in order to capture bed character at shorter length scales; such transects have a similar orientation to the larger basin scale transect and are thus slightly oblique to the palaeoflow of gravity currents entering the basin (SW-NE).

4. Results

4.1 Bed types of the Costa Grande Member

The Castagnola Basin infill has a simple, tabular sheet-like architecture with thinning of the succession towards the basin margins (Fig. 2d). Thinning towards the southern basin margin occurs less abruptly, suggesting that the feeder slope was inclined at a relatively low angle compared to the steeper northern basin margin. Four common bed types were defined in the study interval using a descriptive basis of facies type (sediment texture, composition and structures) and facies arrangement within individual beds, upon which processes associated with sediment transport and deposition were then inferred (Fig. 3).

4.1.1 Type A – Very-thick, stratified mega-beds

Type A beds typically comprise unstratified sandstone, i.e., lacking sedimentary structures, overlain by variably arranged laminated sandstone facies types (e.g., crude wide spaced [<1 cm] planar lamination (*sensu* Talling et al., 2012b)), sub- and super-critical climbing ripple laminations, and less common sinusoidal and current ripple lamination). Inverse and normal grading can be present in a single bed with the former being most common lower within the bed where thin traction carpets (e.g., S2 of Lowe, 1982) and dewatering pipes can also be present. Sole structures (groove casts and prod marks) on the bed base record palaeoflow towards the north-north-east and east whilst ripple lamination within the bed can record more complex and opposing current directions. Erosion at the bed base is common and does not appear to vary significantly across the basin (e.g., Marker Bed 3; Fig. 2d). Mud clasts can be present at the bed base (Clast style 1, Fig. 5) and occur as thin horizons or isolated clasts (Clast style 2, Fig. 5) however MCR divisions (Clast Style 3, Fig. 5) are lacking. Type A beds retain their character and do not pass laterally into other bed types across the study interval (Fig. 2d). Two Type A beds bound the study interval, with several present throughout the Costa Grande Member; they are relatively outsized in terms of their bed thickness compared to other bed types in the study interval (Fig. 4).

Type A beds are interpreted to record deposition from flow which was initially of high concentration with a high rate of sediment fall-out, both of which declined during deposition of the bed (e.g., to produce unstratified sand dominantly overlain by planar and/or climbing ripple lamination; Lowe, 1988; Jobe et al., 2012). The significant thickness of Type A beds may reflect a relatively greater flow duration and/or volume of emplaced sediment, compared to flows depositing other bed types. Sole structures record palaeoflow similar to that found on other bed types and suggest flows entered the basin from a similar direction. Palaeoflow indicators recording complex (multiple direction) flow record the effects of flow confinement during deposition within the Castagnola Basin (e.g., Pickering and Hiscott, 1985; McCaffrey and Kneller, 2001).

4.1.2 Type B – Thick to very-thick, stratified mud-clast-poor beds

Type B beds comprise thick- to very thick-bedded, fine- to medium-grained deposits which typically commence with unstratified sandstone overlain by a range of laminated sandstone facies (Fig. 3). Beds exhibit weak normal grading, (with grading being most pronounced in the upper part of the bed), dewatering structures and convoluted lamination. Sole structures on the bed base record flow towards the north-northeast and east whilst ripple lamination higher within the same bed records more disperse palaeoflow directions often at high angles away from the northern basin margin (Fig. 6). Bed bases can be sharp, planar and apparently non-erosive or erosive at multiple points across the basin with mud clasts concentrated at bed bases (Clast style 1, Fig. 5), some of which are only partially detached from the underlying mudstone. Mud clasts can also occur as distinct horizons, often at the junction between unstratified and stratified sandstone (Clast style 2). Compared to Type C beds, which are also mud-clast-rich, Type B beds have a lower total abundance of mud-clasts with examples of mud clasts still partially attached to the substrate being more common.. Type B beds retain their depositional character laterally (Fig. 8, Bed 215; Fig. 9, Bed 214) but on rare occasions can change laterally and abruptly (<15 m) into Type C bed character (Fig. 10).

Type B beds are interpreted to be the depositional products of aggradation beneath an initial high density turbulent flow *sensu* Lowe (1982) which progressively became less concentrated with time. High rates of suspension fall-out dominated during deposition of the bed (e.g., sinusoidal lamination *sensu* Jobe et al. [2012], dewatered convoluted lamination). Flows were often erosive and, locally, entrained mud clasts from the basin floor however, such entrainment appears to have been less efficient compared to that of Type C beds.. Palaeoflow indicators recording multiple flow directions during deposition of a single bed record the effect of flow confinement during deposition (e.g., Pickering and Hiscott, 1985; McCaffrey and Kneller, 2001).

4.1.3 Type C – Thick to very-thick, variably stratified beds with a co-genetic mud-clast-rich division

At the base of Type C beds unstratified sandstone and or crude widely spaced planar laminated sandstone (*sensu* Talling et al., 2012b), sometimes containing dewatering pipes, pass up into an overlying MCR division (Clast Style 3; Fig. 5) which is in turn overlain by plane parallel and current ripple laminated sandstone at the bed top. The thickness and grain size of Type C beds are comparable to those of the upper range of Type B beds (Fig. 4) and exhibit overall normal grading which is most pronounced in the bed top. Type C bed bases are frequently erosive at multiple sites across the basin floor (Fig. 9; Beds 208, 210) which can include the entrainment of relatively large mud clasts, some of which are still partially attached to the underlying substrate. Sole structures record initial palaeoflow towards the north-northeast and east whilst current ripple lamination, deposited higher (later) within the same bed, records change to more dispersed palaeoflow often at high angles away from the northern confining basin margin (Fig. 6). Mud clasts within the MCR division can sometime develop long axis imbrication consistent with emplacement to the north-east.

Within the MCR division the supporting sandstone matrix can sometimes be subtly more argillaceous (clay-rich) compared to mud-clast-poorer sandstone beneath this MCR division. Individual Type C beds can vary laterally in their depositional character (Fig. 9, Beds 208, 210; Fig. 11, Bed 200) depending upon the thickness of the MCR division or the abundance and size of mud clasts they contain. Thus Type C beds are subdivided into those which contain 1) abundant mud clasts (1 - >100 cm in length) supported within a sandy matrix (Type C1); 2) a higher abundance of similar sized mud clasts supported in a lower volume of sandstone matrix (Type C2); and 3) predominantly significantly large mud clasts, apparently over several metres in length, which can contain sand laminae (Type C3). The size of mud clasts within Type C3 beds can result in very thin sandstones being preserved at their bases and tops, such that the bed can easily be mistaken for a succession of thin-bedded strata (e.g., Bed 200, Fig. 11). Laterally, Type C3 beds can pass into other sub-Type C beds across the basin (e.g., C2, Fig 11, Bed 200) as well as over relatively short length scales (tens of m) in a given outcrop; similar scaled transitions have been documented by Hodgson (2009). Within MCR divisions the sandstone matrix supporting clasts can be irregular in shape, with angular boundaries, and is of comparable grain size to overlying and underlying mud-clast-poorer sandstone in the same bed. The capping laminated sandstone which overlies the MCR division can have undulating lower contacts, being most pronounced in Type C2 beds, and display growth lamination recording syn-depositional loading processes (Fig. 12). Laterally the character (Type C1 to C3) and thickness of MCR divisions can vary significantly (0-140 cm thick) and repeatedly, both on the scale of an individual outcrop (tens to hundreds of m length, Fig. 12) and at the scale of the basin infill and extent of the study interval (>km-scale, Fig. 9). Although uncommon, lateral transition into Type B beds was observed (Fig. 10) whilst transition into Type A and D beds was not observed.

Vertical grain size grading and the repeated association of a relatively mud-clast-poor sandstone, a MCR division and overlying, often loaded, laminated sandstone record the co-genetic association of these facies which were emplaced during a single flow event. Initial deposition of Type C beds was characterised by high rates of sediment fall out from a high concentration flow (e.g., producing unstratified and weakly stratified sandstone at the base of the bed). Late-stage deposition of finer grained well stratified sandstone records a change to deposition beneath relatively lower concentration dilute turbulent flow (e.g., low-density turbidity current *sensu* Lowe, 1982). Palaeoflow indicators recording multiple flow directions during the deposition of a single bed record the effect of flow confinement during deposition. During the change from deposition beneath high to lower concentration flow (i.e., to produce basal unstratified sandstone and capping stratified sandstone, respectively) a co-genetic MCR division was emplaced under flow conditions in which fluid turbulence and bed form generation remained suppressed, presumably by a high concentration of sediment and mud clasts. This distinct, often thick (<140 cm) co-genetic MCR division is somewhat comparable to that found in HEBs described from the distal settings of deep-water systems in relatively less topographically complex settings (e.g., Haughton et al., 2003, 2009; Hodgson, 2009; Talling, 2013), albeit that the former are less argillaceous. Further discussion on the significance and origin of co-genetic MCR divisions follows in section 5.2.

4.1.4 Type D – Very thin to thick well stratified beds

Type D beds are normally graded and are dominated by well stratified sandstones, with planar, sinusoidal, climbing and current ripple laminations (Fig. 3). Dewatering and convolution are easily recognised within these well stratified beds. Occasionally, Type D beds can exhibit complex lamination, with internal truncations, or an unstratified sandstone perched higher within the bed that is not notably coarser grained (Fig. 7). These are the thinnest (<50 cm) and finest grained bed type. Bed bases are rarely erosional and mud clasts are rare and small (<1 cm). Current ripple lamination records dispersed (wide-spreading) palaeoflow directions, often at high angles away from the northern confining basin margin. Type D beds retain their stratified character across the basin and do not transition into other bed types across the study interval.

Type D beds are interpreted to record aggradation beneath low-density turbulent flows (e.g., Bouma, 1962; Lowe, 1982) with lower sediment concentrations compared to those emplacing other bed types. However sinusoidal and climbing ripple lamination indicate that rates of suspension fall-out were still relatively high (e.g., Jobe et al., 2012). Beds containing perched unstratified sandstones have been described adjacent to confining topography in the confined Sorbas Basin, and were interpreted to record reflection of the flow head away from the confining basin margin and subsequent deposition above stratified sandstone recently deposited from the flow body (Haughton, 1994). The origin of this facies arrangement and development of internally truncated lamination sometimes observed in Type D beds is discussed further in sections 5.1 and 5.3, respectively.

4.2 Evolution of palaeoflow in association with a confining basin margin

Flute and prod marks (n=35), current ripple lamination (n=36) and groove casts (n=149) were measured from beds within the study interval. Sole structures (e.g., flutes, grooves and prod marks) indicate that flows entered the basin from the SSW and travelled NNE-ward (Fig. 13, Loc. VII-V) towards the confining counter slope of the northern basin margin where they were deflected (Fig. 13, Loc. IV-I); such change in flow direction can be observed along individual beds (Fig. 9; Beds 208, 210). Current ripple lamination, which can be present higher within the same bed, records palaeoflows that are more variable in direction, either parallel to or more commonly at a high angle away from the strike of the northern basin margin (Fig. 6). Similar observations for different types of palaeoflow indicators have been made in previous studies of the Castagnola Basin (Baruffini et al. 1994; Felletti, 2002) and in a number of confined systems (Kneller et al., 1991; Haughton, 1994; Kneller and McCaffrey, 1999; McCaffrey and Kneller, 2001; Bersezio et al., 2009; Felletti and Bersezio, 2010) and experiments (Kneller et al., 1991). These characteristics are considered to represent contrasting responses of higher and lower concentration portions of the flow (e.g., deflection and reflection, respectively) to confining topography (e.g., Kneller and McCaffrey, 1999). Of the 12 directional sole structures (e.g., flute casts and prod marks) which document a deflected flow direction at the northern basin margin, all record flow deflection to the east. This trend is interpreted to record oblique incidence between flows travelling north-north-east and the east-west strike of the local northern basin margin.

Sole structures recording deflected palaeoflows near the northern basin margin are common in the lower half of the study interval (e.g., below bed 212, Fig. 2d; Package A of Fig. 11) but are not identified stratigraphically higher in the study interval (e.g., above bed 212, Fig. 2d; Package B of Fig. 11). The vertical loss of deflected sole structures is not considered to represent a change from confined to unconfined flow or a different entry point of flows into the basin, because; 1) ripple lamination continues to record wide spread palaeoflow away from the basin margin (Fig. 2d); 2) sole structures indicate that flows still entered the basin from the SSW; and 3) the vertical loss of deflected sole structures does not coincide with a decrease in bed thickness, which might otherwise indicate a change to unconfined settings over a larger depositional area. This vertical change is instead interpreted to represent the effects of basin floor aggradation in a basin with inclined margins, with subsequent migration of the point of onlap both towards and up the basin margins (*sensu* Kneller and McCaffrey, 1999). Thus in a one-dimensional section successive beds record depositional sites which became increasingly farther from the basin margin and sole structure orientation records a change from flow that was deflected to flow that was not yet deflected by the confining topography (Kneller and McCaffrey, 1999). Such migration in the point of basin margin onlap is thought to result in the stratigraphic change in sole structure orientation with deflected sole structures inferred to be located farther north of the outcrop window (e.g., north of Location II). The rapidity with which this change occurs suggests there may have been a terrace or reduction of gradient on the confining slope resulting in a sudden shift in the region of onlap to the north; an uneven gradient was documented on the confining basin margin below the study interval by Felletti (2002). Considering the confinement of gravity currents within the contained Castagnola Basin and previous research on depositional trends adjacent to confining topography (e.g., Barker et al., 2008; Patacci et al., 2014) this study aims to assess how the depositional character of beds containing a co-genetic MCR division varies across the basin and in relation to the downstream confining slope at the northern basin margin.

4.3 Spatial variation of depositional character with respect to a downstream confining basin margin

Correlation of logged sections across the basin allowed the construction of individual bed transects which are orientated approximately NE-SW slightly oblique to the palaeoflow of gravity currents entering the basin (NNE) and highly oblique to both the strike of the northern basin margin (E-W) and flow which was locally deflected towards the east at this location (Fig. 9). The scale of bed transects is largely comparable to the downstream length of the basin (~5 km) at the level of the study interval, as suggested by the overall thinning of the succession at either end of the study interval. Across the basin, maximum grain size remains fairly constant within individual beds with only minor reductions at Location 1 close to the northern basin margin (Beds 208, 210). Bed thickness across the basin typically remains constant (Beds 210, 214) or thickens (Beds 204, 208) prior to eventual thinning and onlap onto the northern basin margin (Beds 204–214); thickness trends show no apparent relation to bed type. A similar increase in bed thickness and sand to mud ratio prior to eventual onlap onto confining topography has been documented in other basins (e.g., Haughton, 1994, 2001; Kneller and McCaffrey, 1999) and in older strata of the Costa Grande Member (Felletti, 2002, 2004a); such characteristics have been attributed to the forced flow deceleration, loss of energy and subsequent sediment deposition on approach to the basin margin.

Beds containing a co-genetic MCR division (Type C) can be present anywhere within the basin with MCR divisions found at least 3.1 km upstream of the northern basin margin (e.g., Fig. 2d; Bed 208, Fig. 9). A MCR division can be present within an individual bed regardless of the change in palaeoflow direction (e.g., incoming or deflected) recorded at the base of the bed (e.g., Beds 208, 210, Fig. 9), with the thickness of this division exhibiting no trend in relation to palaeoflow direction. Laterally the thickness of this division is highly variable (~10-

140 cm) in a non-systematic manner with repeated thickening and thinning occurring both on a basin scale (Fig. 9) as well as on an individual outcrop scale (tens to hundreds of m distance, Fig. 12). Nor does the division in Type C beds exhibit systematic trends in mud clast abundance, as inferred from the dominant bed sub-type at each section, or maximum size with respect to palaeoflow direction or proximity towards the downstream confining counter slope at the northern basin margin. Large mud clasts (>40 cm in length) are found both adjacent to and away from the northern basin margin (e.g., Bed 208, Location II and VII, Fig. 9). Variation in the thickness and character of the co-genetic MCR division, and thus lateral transition between bed sub-types C1 to C3, can occur rapidly and repeatedly and does so non-systematically in relation to palaeoflow direction or proximity to the downstream confining northern basin margin (Fig. 9). Stratigraphically (vertically) there is an apparent concentration of beds containing a MCR division (Type C) at the base of the study interval, however similar deposits are also present in abundance above the study interval.

Despite trends of reducing bed thickness and grain size adjacent to the northern basin margin, bed type and the character of the MCR division within Type C beds exhibit no systematic lateral or stratigraphic variation in relation to palaeoflow direction or proximity towards the downstream counter slope at the northern basin margin. Such findings are in contrast with previous studies concerning the localised distribution of mud-clast and/or clay-rich sandstone facies with respect to confining topography (e.g., Barker et al., 2008; Patacci et al., 2014). The potential causal factors driving the lack of variation in depositional character locally adjacent and towards confining slopes within the Castagnola Basin are explored in Section 5, below.

5. Discussion

5.1 Gravity current confinement and containment within the Castagnola Basin

A number of sedimentological features described in section 4 indicate that gravity currents were both confined and contained within the Castagnola Basin. Containment is directly shown by observations of direct bed onlap onto the basin margin near the base and below the study interval (Felletti, 2002) with thinning of the study interval succession towards the basin margins (Fig. 2d). Sufficiently well-positioned exposure to capture this onlap relationship is lacking throughout the remainder of the study interval. In confined systems significantly thick turbiditic muds are often found above sandstone beds (e.g., ponded muds, Pickering and Hiscott, 1985; Haughton, 1994, 2001); although differentiation between turbiditic and hemipelagic mud could not be made in the Castagnola Basin, thicker mudstones are consistently found above thicker sandstone beds. (e.g., Key Bed 2, Beds 209, 210, Fig. 2d). This relationship suggests that such beds were emplaced by greater volume events, including a greater volume of turbiditic mud, which was contained (ponded) by the physiography of Castagnola Basin. Flow confinement processes are also demonstrated by the variation of palaeoflow along individual beds towards the basin margin, as well as variation between the base and top of the bed, which indicates that flow confinement persisted during bed aggradation. Such trends in palaeoflow have been documented in a number of systems from topographically complex settings (e.g., Pickering and Hiscott, 1985; Kneller et al., 1991; Haughton, 1994; Kneller and McCaffrey, 1999; McCaffrey and Kneller, 2001; Bersezio et al., 2009; Felletti and Bersezio, 2010).

Sedimentary features indicative of high rates of sediment fall-out during deposition (e.g., planar, sinusoidal, climbing ripple lamination and convoluted lamination; Lowe, 1982; Jobe et al., 2012) are frequently described where flow confinement occurs (e.g., Pickering and Hiscott, 1985; Haughton, 1994). In such settings these features likely represent reduced flow carrying capacity (*sensu* Hiscott, 1994a) resulting from flow modification following confinement by sea-floor topography (e.g., Edwards et al., 1994; Kneller and Branney, 1995; Kneller and McCaffrey, 1999). The dominance of these styles of stratification in deposits across the study interval, and the presence of encircling containing basin margins, suggests flows were subject to flow confinement and containment within the Castagnola Basin. Occurrences of complex facies arrangements within individual beds (e.g., perched unstratified sandstone within stratified sandstone), sometimes developed in Type D beds, have previously been documented in deposits from confined systems (e.g., Pickering and Hiscott, 1985; Haughton, 1994, 2001; Sinclair, 1994). Such an arrangement has been attributed to collapse of the flow head away from confining topography with subsequent deposition above recently deposited stratified sandstone from the flow body (e.g., quick beds of Haughton, 1994). Similar deposits in the Castagnola basin are also interpreted to record individual sedimentation events, as bed amalgamation is not observed within the study interval. However as perched, unstratified sandstones do not coincide with significant grain size change in Type D beds these arrangements may instead record fluctuation in local suspension fall-out rate driven by complex flow dynamics within a confined, contained flow following interaction with multiple basin margins (see Section 5.2.3, 5.3) rather than a distinct collapse of the flow head *sensu* Haughton (1994).

5.2 Origin of mud-clast-rich divisions within Type C beds

The following sections evaluate a range of processes capable of emplacing mud-clast-rich strata encased within sandstone, to investigate the origin of the co-genetic MCR division observed within Type C beds.

5.2.1 Modification of the substrate by a succeeding flow event

Where a flow erodes (e.g., Walker, 1966; Fig 14a) or shears (e.g., Butler and Tavarnelli, 2006; Fig. 14b) the underlying muddy substrate and penetrates down to an underlying sandstone bed a composite deposit may result, comprising a MCR division encased within overlying and underlying sandstone. In these cases the MCR division ("ghost bedding" *sensu* Butler and Tavarnelli, 2006) should be traceable laterally into intact mudstone between the separate beds. Neither of these processes are considered plausible formation mechanisms for MCR divisions in the Costa Grande Member, however, as they are never observed to pass laterally into intact mudstone partings (Fig. 9). Additionally, it is unlikely that erosion or deformation would have been capable of affecting the entire thickness of substrate mudstone that frequently exceeds a metre in thickness, across the entire extent of the basin. Furthermore, sandstone overlying MCR divisions tends to be finer grained and laminated, suggesting emplacement by relatively dilute, low concentration flow which would have been incapable of such basin wide erosional effects; bypass of an early high density flow whose presence went unrecorded is unlikely in the small, contained Castagnola Basin.

5.2.2 Gravity current interaction with a confining basin margin

Gravity current-triggered destabilisation of muddy slopes on local sea-floor topography is thought to be capable of triggering secondary synchronous MCR debris flows which might result in the emplacement of sandstone beds containing a distinct MCR division (e.g., McCaffrey and Kneller, 2001). MCR divisions generated in such a manner might be expected to be localised, thicker and perhaps contain larger mud clasts locally adjacent to the slope with which the gravity currents interacted. However MCR divisions in the Costa Grande Member are not localised to the downstream counter-slope at the northern basin margin, and exhibit no distinct trends in terms of frequency, thickness or mud clast size towards this confining feature (Fig. 14c). Although occurrences are rare, long axis imbrication of mud clasts can record emplacement by flow travelling towards the north rather than flow sourced from the north following a failure on the northern basin margin. Basin margin slope instability is considered unlikely as there is a lack of stand-alone slumps or debris flow deposits in the Costa Grande Member (e.g., Baruffini et al., 1994; Felletti, 2002).

Case studies have highlighted the effects that confining sea-floor topography can have through modifying gravity currents as inferred from laterally varying depositional character towards such confining topography (Barker et al., 2008; Patacci et al., 2014). Patacci et al. (2014) describe the localised development and thickening of a MCR division within HEBs with increasing proximity towards a confining slope; such facies development was localised to within 1 km of onlap onto the slope. They consider this facies tract to record the forced deceleration of gravity currents with a compositional and rheological complexity (arising from segregation of mud clasts to the rear of the flow) which was present prior to confinement by the slope and which was captured in the resulting deposits locally adjacent to the slope. The localised effects resulting from confinement by topography, *sensu* Patacci et al. (2014), are not thought to have produced the co-genetic MCR division found in Type C beds, based on their extent across the basin; they are found at least 3.1 km upstream of the northern basin margin, and also based on the lack of systematic variation in their thickness and character towards this margin (Figs. 2d, 9). Furthermore if co-genetic MCR divisions were related to the localised effects of confining slopes, it might be expected that in a suitably located vertical succession such deposits would become less common vertically as the basin infilled and the depositional point became farther away from the point of onlap onto the basin margin (see Section 4.2). However this is not the case and co-genetic MCR divisions are present throughout the Costa Grande Member.

5.2.3 Entrainment and transport of substrate derived mud clasts

Type C beds exhibit substrate erosion and entrainment of mud clasts at multiple sites across the basin (e.g., Fig. 9, Bed 208, Location VII, V; Bed 215, Location VII, V, II) including relatively large mud clasts (> 1 m length), some of which are still partially attached to the underlying mudstone substratum (Fig. 5, Style 1). Such entrainment, which was both voluminous and randomly distributed across the basin floor, is inferred to have established a MCR flow in which mud clasts were unevenly distributed. Such flow character, along with flow containment effects (see section 5.3), is thought to have contributed to the character of the co-genetic MCR division whose presence and thickness within Type C beds varies both significantly and non-systematically in downstream and cross-flow directions. Entrainment of the muddy substrate into the flow is frequently cited as a mechanism initiating the development of those hybrid flows which emplace HEBs containing a distinctly thick co-genetic MCR division (e.g., Haughton et al., 2003, 2009; Talling et al., 2004; Amy and Talling, 2006; Davis et al., 2009; Patacci et al., 2014), comparable to that within Type C beds.

In Type C beds mud clasts are more abundant, reach a greater maximum size (>1 m) and are concentrated into distinct, often thick (<1.4 m), co-genetic MCR divisions compared to mud clasts in Type A and B beds. As all these beds exhibit erosive bases and partial entrainment of large pieces of muddy substrate, Type C flows are thought to have been distinct in that they were more efficient at entraining muddy substrate, limiting mud clast diminution during transport and/or supporting and concentrating mud clasts within the flow. Coarse grain sizes and less frequent examples of partial substrate entrainment compared to other bed types suggests Type C flows may have been more efficient at entraining substrate from the basin floor. The relative dominance of unstratified sandstone in the lower parts of Type C beds suggests flows were of relatively higher sediment concentration, in which fluid turbulence would have been more suppressed (e.g., Lowe, 1988) and rates of mud clast breakup lower (e.g., Smith, 1972), compared to those in relatively lower concentration flows emplacing better stratified deposits (e.g., Type A and B beds). Although a wide range of mud clast shapes (e.g., sub-rounded to angular) are found in Type C beds, angular examples are relatively common compared to other bed types. However angular clasts do not directly indicate reduced clast breakup within Type C flows, as angular mud clasts can be released into the flow during the transportation and break-up of larger mud clasts (Fig. 8). Furthermore the evolution of mud clast characteristics (e.g., size and shape) is expected to be influenced by a number of factors whose relative importance and interplay during the flow event are poorly understood. For example mud clast size and shape can be influenced both by the intensity of fluid turbulence and duration of transport within the flow; both of which may act in combination or in opposition in the flow (Smith, 1972). Thus it is difficult to constrain which of efficient entrainment or limited mud clast breakup was more influential in the development of co-genetic MCR divisions within Type C beds.

The elevation of the co-genetic MCR division within Type C beds, emplaced by aggradation (see section 4.1), suggests mud clasts were retained within the flow whilst the underlying mud-clast poorer sandstone was deposited. Mud clasts may have been located within a more rearward later depositing region of the flow, perhaps following longitudinal fractionation processes during flow run-out (see Haughton et al., 2003). However, considering the recent entrainment of mud clasts and limited available flow run-out distance across the basin floor (< 5 km), such rearward segregation may have been relatively incomplete and as such may not have been the dominant process driving the concentration of mud clasts into the co-genetic MCR divisions. Perhaps more influential were processes which provided mud clast support within high concentration flow (e.g., mud clast buoyancy, hindered settling and kinetic sieving) whilst deposition of much of the sand fraction occurred. Mud clasts are positively buoyant when their often relatively low density is exceeded by that of the surrounding sediment-water mixture (e.g., Flemings et al., 2006; Talling et al., 2010). High rates of sediment fall-out typical of high concentration flows (Lowe, 1988) can drive a significant upwards flux of displaced fluid which may hinder the settling of other particles (e.g., hindered settling; Davis, 1968; Druitt, 1995); mud clasts may have been preferentially supported due to their larger surface areas compared to sand grains. Displacement of mud clasts upwards through the flow can also occur in high concentration flows as smaller sand particles are more likely to fall into voids and thus settle downwards whilst larger mud clasts settle less freely (e.g., kinetic sieving; Bridgwater, 1976; Gray et al., 2006). Similar mechanisms were proposed to provide mud clast support in the experiments of Postma (1988) which demonstrated that mud clasts, including outsize examples, could be elevated and concentrated in a flow and transported at a density interface between an underlying high concentration low turbulence layer and overlying lower concentration more turbulent layer. With sand deposition and subsequent reduction of flow concentration beneath a critical threshold, mud clast support mechanisms associated with higher concentration flow would have been subdued or removed, resulting in the deposition of a co-genetic MCR division above mud-clast poorer sandstone in the same bed. A sudden increase in sediment fall-out rate, reduction in flow concentration and deposition of mud clasts may have been triggered by the effects of reduced flow confinement (e.g., Kneller and McCaffrey, 1999) within the Castagnola Basin (see section 5.3).

Although Type C beds record deposition beneath a high concentration weakly- to non-turbulent sandy flow, they are considered to be distinct from high density turbidites (e.g., Lowe, 1988), which typically contain much thinner or absent mud clast horizons. Type C beds are somewhat more comparable to HEBs as described by Haughton et al. (2003, 2009) and Talling (2013), which also contain a distinct thick co-genetic MCR division overlying relatively mud-clast-poor sandstone within the same bed. However, they differ in that the supporting sandstone matrix within the co-genetic MCR division is not as argillaceous as that described by those authors, and is thus not considered to have been deposited beneath a region of notably more cohesive flow within the flow event (e.g., Haughton et al., 2003, 2009; Talling, 2013). The relatively cleaner (clay-poor) nature of the matrix within Type C co-genetic MCR divisions may reflect the relatively recent entrainment, shorter flow run-out distance and limited disaggregation of mud clasts within the contained Castagnola Basin compared to the larger flow run-out distances achieved in the uncontained systems from which HEBs with more argillaceous co-genetic MCR divisions have hitherto been described (e.g., Haughton et al., 2003, 2009; Amy and Talling, 2006; Davis et al., 2009; Hodgson, 2009). Thus the term sandy-HEB is used here for beds containing a thick, co-genetic MCR division with a relatively non-argillaceous sandstone matrix that may also exhibit significant, non-systematic lateral variability in terms of its presence, thickness and character; it can pass into mud-clast-poorer sandstone. Flows emplacing such deposits may represent the early stages of hybrid flow development (*sensu* Haughton et al., 2003, 2009).

5.3 Influence of flow containment upon deposit character and distribution in confined deep-water systems

The lack of localised systematic trends in depositional character near to confining topography within the CC Castagnola Basin is in contrast to that documented by Barker et al. (2008) and Patacci et al. (2014) in CU settings. The following section assesses the importance of flow containment (ponding), in addition to flow confinement, in CC settings and its possible influence upon gravity flow dynamics and deposit character and distribution within topographically complex settings.

5.3.1 Processes of flow confinement

Considerable experimental work has explored the interaction of gravity currents and topography (Pantin and Leeder, 1987; Edwards et al., 1994; Kneller, 1997; Kneller and McCaffrey, 1999; Lamb et al., 2004, 2006; Toniolo et al., 2006a,b; Sequireos et al., 2009). Many have shown how disturbances, characterised by downstream changes in flow velocity and thickness, are generated locally where flows are obstructed by a confining obstacle (e.g., Pantin and Leeder, 1987; Edwards et al., 1994; Kneller, 1997; Lamb et al., 2004, 2006; Toniolo et al., 2006a,b; Sequireos et al., 2009). Such topographically induced flow non-uniformity (*sensu* Kneller and Branney, 1995) can be associated with a reduced sediment carrying capacity and enhanced sediment fall-out rate from the flow (e.g., Kneller and McCaffrey, 1999). Where flow containment occurs in addition to flow confinement (Fig. 1), such as that in the Castagnola Basin, this induced flow non-uniformity effects may extend across the entire basin (e.g., Pantin and Leeder, 1987; Kneller, 1991; Alexander and Morris, 1994; Kneller and McCaffrey, 1995; Lamb et al., 2004, 2006; Toniolo et al., 2006a,b). Features associated with high sediment fall-out rates are dominant in deposits across the Castagnola Basin (e.g., deposition of unstratified sandstone and development of crude, planar and sinusoidal lamination) and may reflect such non-uniformity effects and/or the effects of limited flow expansion and dilution in such settings (e.g. Middleton, 1967; Scheidegger and Potter, 1971; Garcia, 1994).

Both experimental and outcrop studies have demonstrated how complex multi-directional flow is established where flows interact with and are confined by a single topographic feature (e.g., Kneller et al., 1991; Haughton, 1994; Kneller and McCaffrey, 1999; Amy et al., 2004). Kneller and McCaffrey (1999) show how confinement of a density-stratified flow can result in the reflection of the upper dilute layer at a high angle to the strike of the counter slope, whilst the basal higher concentration layer is deflected laterally, parallel to the strike of the slope. Such palaeoflow trends recording complex three dimensional flow dynamics have been documented in outcrop studies (Kneller et al., 1991; McCaffrey and Kneller, 2001) including the Castagnola Basin (Felletti, 2002; this study Figs. 6, 12). Furthermore, where the incidence angle with the confining obstacle is oblique, such as in the Castagnola Basin, the flow reflected perpendicularly away from the counter slope is both oblique to the deflected dense basal layer as well incoming flow still entering the basin (e.g., Kneller et al., 1991; McCaffrey and Kneller, 2001; see Fig. 15).

However the majority of experimental studies have generally focussed upon flow interaction with a single confining slope (CU setting) and consequently largely fail to explore how the three dimensional flow dynamics of a confined flow might evolve in CC settings. However, in the oblique-incidence experiments of Kneller et al. (1991), the reflected flow triggered by the initial downstream confinement travelled towards and interacted with the side wall of the tank. Thus in CC settings it is probable that reflected and deflected flows generated from initial interaction with a confining basin margin may further interact with; 1) other basin margins (Kneller et al., 1991); 2) other flow disturbances generated at these margins, such as that observed from “sloshing” liquids in transportation vessels (e.g., Bryant and Stiassnie, 1995; Faltinsen et al., 2005); and 3) flow still entering the basin (Pantin and Leeder, 1987; Edwards et al., 1994). The oblique incidence with a downstream confining basin margin and presence of encircling confining topography in the Castagnola Basin would have favoured such complex three dimensional flow dynamics. This, along with voluminous local entrainment of muddy substrate, may have resulted in the lack of any systematic depositional trends across the basin.

Distinct sedimentary structures (e.g., biconvex rounded ripples and small-scale hummocky type lamination with internal truncations) have been suggested to provide evidence of multi-directional flow adjacent to confining topography in deep-water CU systems (Tinterri, 2011). The lack of such structures in the Castagnola Basin is believed to reflect the high sediment fall-out rates and/or complexity of multi-directional flow dynamics. With high sediment fall-out rates bed aggradation outpaces traction and bed forms preferentially develop low relief long wavelength stratification (Lowe, 1988; Jobe et al., 2012) which is a poor indicator of palaeoflow. Instances when internally truncated stratification does occur, in thinner bedded, finer grained, better stratified Type D beds (Fig. 7), suggest formation where the flow concentration and sediment fall-out rate were relatively lower. In the presence of highly complex three dimensional flow, such as that thought to occur in the Castagnola Basin, the lack of a long-established flow direction may also hinder the development ripple and other asymmetrical bed forms capable of recording multi-directional flow (see Yokokawa, 1995, Yokokawa et al., 1995).

6. Conclusions

Gravity currents entering the Castagnola Basin were subject to deflection and reflection following oblique incidence with a downstream confining counter slope at the northern basin margin and were fully contained by encircling basin margins. Bed-to-bed correlations orientated at a high angle to the strike of the downstream northern basin margin show the distribution and depositional character of sandy HEBs (Type C beds) over short (<100 m) and long (<5 km) length scales. Individual bed transects demonstrate that sandy HEBs are extensive (>3 km) across the basin and are highly variable laterally in terms of the presence and thickness of a co-genetic MCR division, as well as the size and abundance of mud clasts within this division, over short (tens of m) and longer (< km) length scales. Such variation is non-systematic with respect to palaeoflow direction and with increasing proximity towards confining sea-floor topography. The extensive and non-systematic variable character of sandy HEBs within the CC Castagnola Basin setting is in contrast to similar deposits from CU settings, where systematic depositional trends have been recognised locally near to confining sea-floor topography (e.g., Barker et al., 2008; Patacci et al., 2014).

Distinct co-genetic MCR divisions, which exhibit highly variable and non-systematic variation in depositional character and distribution with respect to their distance from confining topography, are interpreted to have resulted from the volume, support and uneven distribution of abundant mud clasts in high concentration flows. Flow containment, in addition to flow confinement, is thought to have established extensive complex three dimensional flow dynamics across the basin, following interaction with multiple basin margins, which perturbed the development of localised or coherent depositional trends adjacent to confining topography.

This study sheds light on the contrasts in HEB distribution and depositional trends between different topographically complex settings; specifically showing that HEBs are not necessarily localised adjacent to confining topography and can vary non-systematically in their depositional character in systems where the effects of flow containment were superimposed upon those of flow confinement. These insights highlight the importance of understanding the confined system type (e.g., contained or uncontained) and have implications for the prediction of depositional character, and thus reservoir quality distribution, in topographically complex settings.

Acknowledgments

This research was funded by the Turbidites Research Group industry consortium (Anadarko, BG Group, BP, ConocoPhillips, Dana Petroleum, Maersk Oil, Nexen, OMV, Petronas, Statoil, Tullow Oil and Woodside). We gratefully acknowledge the support of Francesca Porro and Roberta Meneghin from the University of Milan for assisting in field data collection.

References

Athmer, W., Luthi, S.M., 2011. The effect of relay ramps on sediment routes and deposition: A review. Sedimentary Geology 242, 1-17.

Alexander, J., Morris, S., 1994. Observations on Experimental, Non channelized High-Concentration Turbidity Currents and Variations in Deposits around Obstacles. Journal of Sedimentary Research 64, 899-909.

Amy, L.A., McCaffrey, W.D., Kneller, B.C., 2004. The influence of a lateral basin-slope on the depositional patterns of natural and experimental turbidity currents. In: Joseph, P., Lomas, A. (Eds), Deep-Water Sedimentation in the Alpine Basin of SE France. Geological Society Special Publication 221, Geological Society of London, London, pp. 311-330.

Amy, L.A., Talling, P.J., 2006. Anatomy of turbidites and linked debrites based on long distance (120 x 30 km) bed correlation, Marnoso Arenacea Formation, Northern Apennines, Italy. Sedimentology 53, 161-212.

Andreoni, G., Galbiati, B., Maccabruni, A., Vercesi, P.L., 1981. Stratigrafia e paleogeografia dei depositi oligocenici sup. – miocenici inf. nell'estremità orientale del bacino ligure-piemontese. Rivista Italiana di Paleontologia e Stratigrafia 87, 245-282.

Armentrout, J.M., Kanschat, K.A., Meisling, K.E., Tsakma, J.J., Antrim, L., McConnell, D.R., 2000. Neogene turbidite systems of the Gulf of Guinea continental margin slope, offshore Nigeria. In: Bouma, A.H., Stone, C.G. (Eds) Fine-Grained Turbidite Systems: American Association of Petroleum Geologists, Memoir 72/SEPM, Special Publication 68, pp. 93–108.

Barker, S.P., Haughton, P.D.W., McCaffrey, W.D., Archer, S.G., Hakes, B., 2008. Development of rheological heterogeneity in clay-rich high-density turbidity currents: Aptian Britannia Sandstone Member, UK continental shelf. Journal of Sedimentary Research 78, 45-68.

Baruffini, L., Cavalli, C., Papani, L., 1994. Detailed stratal correlation and stacking patterns of the Gremiasco and lower Castagnola turbidite systems, Tertiary Piedmont Basin, northwestern Italy. In: Weimer, P., Bouma, A.H., Perkins, B.F. (Eds) 15th Annual Research Conference Submarine Fans and Turbidite Systems. Society of Economic Palaeontologists and Mineralogists, Gulf Coast Section, pp. 9-21.

Bersezio, R., Felletti, F., Riva, R., Micucci, L. 2009. Bed thickness and facies trends of turbiditic sandstone bodies. Unravelling the effects of basin confinement, depositional processes and modes of sediment supply. In: Kneller, B., Martinsen, O.J., McCaffrey, B. (Eds.) External Controls on Deep-Water Depositional Systems. SEPM Special Publication 92, pp. 303-321.

Biella, G.C., Clari, P., De Franco, R., Gelati, R., Ghibaudo, G., Gnaccolini, M., Lanza, R., Polino, R., Ricci, B., Rossi, P.M., 1992. Geometrie crostali al nodo Alpi/Appennino: conseguenze sull'evoluzione cinematica dei bacini neogenic. 76 Congresso Societa Geologica Italian, Abstracts, 192-195.

Bouma, A.H., 2000. Coarse-grained and fine-grained turbidite systems as end member models: applicability and dangers. Marine and Petroleum Geology 17, 137-143.
Bridgwater, J., 1976. Fundamental powder mixing mechanisms. Powder Technology 15, 215-236.
Brunt, R.L., McCaffrey, W.D., Kneller, B.C., 2004. Experimental modelling of the spatial distribution of grain size developed in a fill-and-spill mini-basin setting. Journal of Sedimentary Research 74, 438-446.
Bryant, P.J., Stiassnie, M., 1995. Water waves in a deep square basin. Journal of Fluid Mechanics 302, 65-90.
Butler, R.W.H., Tavarnelli, E., 2006. The structure and kinematics of substrate entrainment into high-concentration sandy turbidites: a field example from the Gorgoglione 'flysch' of southern Italy. Sedimentology 53, 655-670.
Cavanna, F., Di Guilio, A., Galbiati, B., Mosna, S., Perotti, C.R., Pieri, M., 1989. Carta geologica dell'estremità orientale del Bacino Terziario Ligure Piemontese. Atti Ticinensi di Scienze della Terra 32, pp. 1-22.
Choux, C.M.A., Baas, J.H., McCaffrey, W.D., Haughton, P.D.W., 2005. Comparison of spatio-temporal evolution of experimental particulate gravity flows at two different initial concentrations, based on velocity, grain size and density data. Sedimentary Geology 179, 49-69.
Davies, R., 1968. The experimental study of the differential settling of particles in suspension at high concentrations. Powder Technology 2, 43-51.
Davis, C., Haughton, P.D.W., McCaffrey, W.D., Scott, E., Hogg, N., Kitching, D. 2009. Character and distribution of hybrid sediment gravity flow deposits from the outer Forties Fan, Palaeocene Central North Sea, UKCS. Marine and Petroleum Geology 26, 1919-1939.
Di Giulio, A., Galbiati, B., 1993. Escursione nell'estremità orientale del Bacino Terziario Piemontese. Interazione tettonica-eustatismo nella sedimentazione di un bacino tardo-post orogenico. 3 Convegno del Gruppo Informale di Sedimentologia del CNR, pp. 1-28.
Druitt, T.H., 1995. Settling behaviour of concentrated dispersions and some volcanological applications. Journal of Volcanology and Geothermal Research 65, 27-39.
Edwards, D.A., Leeder, M.R., Best, J.L., Pantin, H.M., 1994. On experimental reflected density currents and the interpretation of certain turbidites. Sedimentology 41, 437-461.
Faltinsen, O.M., Rognebakke, O.F., Timokha, A.N., 2005. Classification of three-dimensional nonlinear sloshing in a square-base tank with finite depth. Journal of Fluids and Structures 20, 81-103.
Felletti, F., 2002. Complex bedding geometries and facies associations of the turbiditic fill of a confined basin in a transpressive setting (Castagnola Fm.,Tertiary Piedmont Basin, NW Italy). Sedimentology 49, 645-667.
Felletti, F., 2004a. Spatial variability of Hurst statistics in the Castagnola Formation, Tertiary Piedmont Basin, NW Italy: discrimination of sub-environments in a confined turbidite system. Geological Society of London Special Publications, 222, 285-305.

Felletti, F., 2004b. Statistical modelling and validation of correlation in turbidites: an example from the Tertiary Piedmont Basin (Castagnola Fm., Northern Italy). Marine and Petroleum Geology 21, 23-39.

Felletti F., Bersezio, R., 2010. Quantification of the degree of confinement of a turbidite-filled basin: a statistical approach based on bed thickness distribution. Marine and Petroleum Geology 27, 515–532.

Fisher, R.V., 1971. Features of coarse-grained, high-concentration fluids and their deposits. Journal of Sedimentary Research 41, 916-927.

Flemings, P.B., Behrmann, J.H., John, C.M., 2006. Gulf of Mexico Hydrogeology. Proceeding of the International Ocean Drilling Program, 308, College Station, Texas, USA.

Gamberi, F., Rovere, M., 2011. Architecture of a modern transient slope fan (Villafranca fan, Gioia basin - Southeastern Tyrrhenian Sea). Sedimentary Geology 236, 211-225.

Garcia, M., Parker, G., 1993. Experiments on the entrainment of sediment into suspension by dense bottom current. Journal of Geophysical Research 98, 4793-4807.

Garcia, M., 1994. Depositional Turbidity Currents Laden with Poorly Sorted Sediment. Journal of Hydraulic Engineering 120, 1240-1263.

Gray, J., Chugunov, V.A., 2006. Particle-size segregation and diffusive remixing in shallow granular avalanches. Journal of Fluid Mechanics 569, 365-398.

Hampton, M.A., 1972. The role of subaqueous debris flow in generating turbidity currents. Journal of Sedimentary Research 42, 775-793.

Haughton, P.D.W., 1994. Deposits of Deflected and Ponded Turbidity Currents, Sorbas Basin, Southeast Spain. Journal of Sedimentary Research 64, 233-246.

Haughton, P., 2001. Contained turbidites used to track sea bed deformation and basin migration, Sorbas Basin, south-east Spain. Basin Research 13, 117-139.

Haughton, P.D.W., Barker, S.P., McCaffrey, W.D., 2003. 'Linked' debrites in sand-rich turbidite systems - origin and significance. Sedimentology 50, 459-482.

Haughton, P., Davis, C., McCaffrey, W., Barker, S., 2009. Hybrid sediment gravity flow deposits - Classification, origin and significance. Marine and Petroleum Geology 26, 1900-1918.

Hiscott, R.N., 1994. Loss of Capacity, Not Competence, as the Fundamental Process Governing Deposition from Turbidity Currents. Journal of Sedimentary Research 64, 209-214.

Hiscott, R.N., 1994. Traction-carpet stratification in turbidites-fact or fiction? Journal of Sedimentary Research 64, 204-208.

Hodgson, D.M., 2009. Distribution and origin of hybrid beds in sand-rich submarine fans of the Tanqua depocentre, Karoo Basin, South Africa. Marine and Petroleum Geology 26, 1940-1956.

Ibbeken, H., 1978. The Nivione structure: contemporaneous tectonics and sedimentation between the Ligurian and Tuscan Orogenies. In Alps, Appennines, Hellenides, Scientific Reports n.38; Inter-Union Commission of Geodynamics, pp. 274-275.

Jackson, C.A., Johnson, H.D., 2009. Sustained turbidity currents and their interaction with derbite-related topography; Labuan Island, offshore NW Borneo, Malaysia. Sedimentary Geology, 219, 77-96.

Jobe, Z.R., Lowe, D.R., Morris, W.R., 2012. Climbing-ripple successions in turbidite systems: depositional environments, sedimentation rates and accumulation times. Sedimentology 59, 867-898.

Kneller, B.C., Branney, M.J., 1995. Sustained High-Density Turbidity Currents and the Deposition of Thick Massive Sands. Sedimentology 42, 607-616.

Kneller, B.C., McCaffrey, W.D., 1995. Modelling the effects of salt-induced topography on deposition from turbidity currents. Society of Economic Palaeontologists and Mineralogists, Gulf Coast Section, pp. 137-145.

Kneller, B., McCaffrey, W., 1999. Depositional effects of flow nonuniformity and stratification within turbidity currents approaching a bounding slope: Deflection, reflection, and facies variation. Journal of Sedimentary Research 69, 980-991.

Kneller, B., Buckee, C., 2000. The structure and fluid mechanics of turbidity currents: a review of some recent studies and their geological implications. Sedimentology 47, 62-94.

Kneller, B., Edwards, D., McCaffrey, W., Moore, R., 1991. Oblique Reflection of Turbidity Currents. Geology 19, 250-252.

Kneller, B.C., Bennett, S.J., McCaffrey, W.D., 1997. Velocity and turbulence structure of density currents and internal solitary waves: potential sediment transport and the formation of wave ripples in deep water. Sedimentary Geology 112, 235-250.

Kuenen, P.H., 1966. Experimental Turbidite Lamination in a Circular Flume. Journal of Geology 74, 523-545.

Lamb, M.P., Hickson, T., Marr, J.G., Sheets, B., Paola, C., Parker., G. 2004. Surging versus continuous turbidity currents: Flow dynamics and deposits in an experimental intraslope minibasin. Journal of Sedimentary Research 74, 148-155.

Lamb, M.P., Toniolo, H., Parker, G., 2006. Trapping of sustained turbidity currents by intraslope minibasins. Sedimentology 53, 147-160.

Lowe, D.R., 1982. Sediment Gravity Flows .2. Depositional Models with Special Reference to the Deposits of High-Density Turbidity Currents. Journal of Sedimentary Petrology 52, 279-298.

Lowe, D.R., 1988. Suspended-load fallout rate as an independent variable in the analysis of current structures. Sedimentology 35, 765-776.

Madof, A.S., Christie-Blick, N., Anders, M.H., 2009. Stratigraphic controls on a salt-withdrawal intraslope minibasin, north-central Green Canyon, Gulf of Mexico: Implications for misinterpreting sea level change. AAPG Bulletin 93, 535-561.

Maino, M., Decarlis, A., Felletti, F., Seno, S., 2013. Tectono-sedimentary evolution of the Tertiary Piedmont Basin (NW Italy) within the Oligo-Miocene central Mediterranean geodynamics. Tectonics 32, 593-619.

McCaffrey, W., Kneller, B., 2001. Process controls on the development of stratigraphic trap potential on the margins of confined turbidite systems and aids to reservoir evaluation. AAPG Bulletin 85, 971-988.

Middleton, G.V., 1967. Experiments on density and turbidity currents: III. Deposition of sediment. Canadian Journal of Earth Sciences 4, 475-505.

Middleton, G.V., Southard, J.B., 1984. Mechanics of sediment movement. Society of Economic Palaeontologists and Mineralogists Short Course Notes 3, pp. 401pp.

Muzzi Magalhaes, P., Tinterri, R., 2010. Stratigraphy and depositional setting of slurry and contained (reflected) beds in the Marnoso-arenacea Formation (Langhian-Serravallian) Northern Apennines, Italy. Sedimentology 57, 1685-1720.
Pantin, H.M., Leeder, M.R., 1987. Reverse Flow in Turbidity Currents - the Role of Internal Solitons. Sedimentology 34, 1143-1155.
Patacci, M., Haughton, P.D.W., McCaffrey, W.D., 2014. Rheological Complexity in Sediment Gravity Flows Forced to Decelerate against a Confining Slope, Braux, SE France. Journal of Sedimentary Research 84, 270-277.
Pickering, K.T., Hiscott, R.N., 1985. Contained (Reflected) Turbidity Currents from the Middle Ordovician Cloridorme Formation, Quebec, Canada - an Alternative to the Antidune Hypothesis. Sedimentology 32, 373-394.
Postma, G., Nemec, W., Kleinspehn, K.L., 1988. Large Floating Clasts in Turbidites - a Mechanism for Their Emplacement. Sedimentary Geology 58, 47-61.
Ricci Lucchi, F., Valmori, E, 1980. Basin-wide turbidites in a Miocene, over-supplied deep-sea plain: a geometrical analysis. Sedimentology 27, 241-270.
Ricci Lucchi, F.R., 1986. The Oligocene to Recent foreland basins of the northern Apennines. In Allen, P.A., Homewood, P. (Eds), Foreland basins. International Association of Sedimentologists Special Publication 8, 105-139.
Scheidegger, A.E., Potter, P.E., 1971. Down current decline of grain size and thickness of a single turbidite bed: a semi-quantitative analysis. Sedimentology 17, 41-49.
Sequeiros, O.E., Cantelli, A., Viparelli, E., White, J.D.L., Garcia, M.H., Parker, G., 2009. Modelling turbidity currents with nonuniform sediment and reverse buoyancy. Water Resources Research 45, 1-28 10.1029/2008WR007422
Sinclair, H.D., 1994. The Influence of Lateral Basinal Slopes on Turbidite Sedimentation in the Annot Sandstones of Se France. Journal of Sedimentary Research 64, 42-54.
Smith, N.D., 1972. Flume experiments on the durability of mud clasts. Journal of Sedimentary Research 42, 378-383.
Stacey, M.W., Bowen, A.J., 1988. The vertical structure of turbidity currents and a necessary condition for self-maintenance. Journal of Geophysical Research 93, 3543-3553.
Stocchi, S., Cavalli, C., Baruffini, L., 1992. The Guaso (south-central Pyrenees), Gremiasco and Castagnola (eastern sector of Tertiary Piedmont basin) turbidite deposits: Geometry and detailed correlation pattern. Atti Ticinensi di Scienze della Terra 35, 153-177.
Sylvester, Z., Lowe, D.R., 2004. Textural trends in turbidites and slurry beds from the Oligocene flysch of the East Carpathians, Romania. Sedimentology 51, 945-972.
Talling, P.J., 2013. Hybrid submarine flows comprising turbidity current and cohesive debris flow: Deposits, theoretical and experimental analyses, and generalized models. Geosphere 9, 460-488.
Talling, P.J., Amy, L.A., Wynn, R.B., Peakall, J., Robinson, M., 2004. Beds comprising debrite sandwiched within co-genetic turbidite: origin and widespread occurrence in distal depositional environments. Sedimentology 51, 163-194.

Talling, P.J., Amy, L.A., Wynn, R.B., Blackbourn, G., Gibson, O., 2007. Evolution of turbidity currents deduced from extensive thin turbidites: Marnoso Arenacea Formation (Miocene), Italian Apennines. Journal of Sedimentary Research 77, 172-196.

Talling, P.J., Wynn, R.B., Schmmidt, D.N., Rixton, R., Sumner, E., Amy, L., 2010. How Did Thin Submarine Debris Flows Carry Boulder-Sized Intraclasts for Remarkable Distances across Low Gradients to the Far Reaches of the Mississippi Fan? Journal of Sedimentary Research 80, 829-851.

Talling, P.J., Malgesini, G., Sumner, E.J., Amy L.A., Felletti, F., Blackbourn, G., Nutt, C., Wilcox, C., Harding, I.C., Khan, S., 2012a. Planform geometry, stacking pattern, and extra-basinal origin of low-strength and intermediate-strength cohesive debris flow deposits in the Marnoso-arenacea Formation. Geosphere 8, 1-24.

Talling, P.J., Masson, D.G., Sumner, E.J., Malgesini, G., 2012b. Subaqueous sediment density flows: Depositional processes and deposit types. Sedimentology 59, 1937-2003.

Toniolo, H., Lamb, M., Parker, G., 2006a. Depositional turbidity currents in diapiric minibasins on the continental slope: Formulation and theory. Journal of Sedimentary Research 76, 783-797.

Toniolo, H., Parker, G., Voller, V., Beaubouef, R.T., 2006b. Depositional turbidity currents in diapiric minibasins on the continental slope: Experiments - Numerical simulation and upscaling. Journal of Sedimentary Research 76, 798-818.

Tinterri, R., 2011. Combined flow sedimentary structures and the genetic link between sigmoidal and hummocky cross-stratification. GeoActa (Bologna) 10 1-43.

Van Andel, T.H., Komar, P.D., 1969. Ponded Sediments of the Mid-Atlantic Ridge between 22° and 23° North Latitude. Geological Society of America Bulletin 80, 1163-1190.

Walker, R.G., 1966. Shale Grit and Grindslow Shales - Transition from Turbidite to Shallow Water Sediments in Upper Carboniferous of Northern England. Journal of Sedimentary Petrology 36, 90-114.

Yokokawa, M., 1995. Combined-flow ripples: genetic experiments and applications for geologic records. Kyushu University, Faculty of Science, Memoirs, Series D, Earth and Planetary Sciences 29, 1-38.

Yokokawa, M., Masuda, F., Endo, N., 1995. Sand particle movement on migrating combined-flow ripples. Journal of Sedimentary Research 65, 40-44.

Figure Captions

Fig. 1. Schematic plan view depicting the difference between unconfined and uncontained (A), confined and uncontained (B) and confined and contained (C) deep-water systems. (A) Sediment gravity flows and the depositional systems they emplace are free to expand in unconfined uncontained settings due to the absence of confining sea-floor topography. (B, C) In the presence of confining sea-floor topography flows and depositional systems are modified (confined) and may be additionally contained in the presence of suitable encircling confining sea-floor topography (C only).

Fig. 2. (A) Stratigraphy (after Andreoni et al., 1981), (B) sketch cross-section (after Di Giulio and Galbiati, 1993) and (C) geological sketch map (redrawn and modified after Stocchi et al., 1992) of the Castagnola Basin with inset showing its location in the eastern portion of the Tertiary Piedmont Basin of north west Italy (modified after Felletti, 2002a). (D) Correlation of log transects across the Costa Grande Member study interval, log positions indicated on (C).

Fig. 3. Bed types recognised within the Costa Grande Member study interval.

Fig. 4. Graph depicting bed type maximum grain size versus bed thickness. Type A beds are outsized in terms of their thickness compared to other bed types whilst Type D beds are thinner bedded and finer grained. The ranges of bed thickness and grain size in Type B and C beds overlap with the latter bed type being thicker and coarser grained. Sand grain size abbreviations are as follows: Lvf, lower very fine; Uvf, upper very fine; Lf, lower fine; Uf, upper fine; Lm, lower medium; Um, upper medium.

Fig. 5. Key characteristics of the different styles of mud clast distribution observed within deposits of the Costa Grande Member.

Fig. 6. Palaeoflow data collected all bed types within the study interval. Sole structures (groove casts, prod marks and flute casts) record two distinct trends with incoming flow directed north-north-east towards the confining northern margin of the Castagnola Basin and flow which was deflected eastwards at this northern basin margin. Current ripple lamination, representing later stage deposition after sole structure formation, records wider spread palaeoflow directions which are often directed at a high angle away from the confining northern basin margin.

Fig. 7. (A) Internally complex and truncated lamination within a Type D bed. (B) Vertically alternating stratified and unstratified sandstone within a Type D bed dominated by sinusoidal lamination in the upper half of the bed.

Fig. 8. Short length-scale transect through a Type B bed at Location II with partial entrainment of muddy substrate along the base of the bed. Type B beds retain their depositional character over short length-scales compared to Type C beds (see Figs. 9, 12).

Fig. 9. Basin scale transects of individual bed types across the Costa Grande Member study interval. Type B and D beds retain their depositional character across the basin whilst Type C beds are highly variable in terms of the thickness of their co-genetic mud-clast-rich divisions and the size and abundance of mud clasts within this division. Co-genetic mud-clast-rich divisions are extensive across the basin (>5 km) and variation in their character is non-systematic in respect to palaeoflow direction and proximity towards the confining northern basin margin.

Fig. 10. Example of lateral transition from a Type B (right) to a Type C2 (left) bed character over <15m. Typically Type B beds retain their depositional character on outcrop (Fig. 4) and basin (Fig. 9; Bed 214) scales whilst Type C beds typically vary between Type C sub-types (Figs. 9; Bed 208, 210).

Fig. 11. Lateral variation in the size and abundance of mud clasts can result in significant variation in the character of the co-genetic mud-clast-rich division (e.g., Beds 200, 201) and overall bed character. Sub-type C3 is rare (e.g., Bed 200 only) and comprises significantly large mudstone rafts (>1 metre length) which result in the supporting sandstone matrix being sparse and irregular in shape; sub-type C3 in Bed 200 is seen to pass laterally into sub-type C2 along a single continuous outcrop (Location V) within a distance of 30 m (not shown).

Fig. 12. Short length-scale transect through a Type C bed at Location IV illustrating how the thickness of the co-genetic mud-clast-rich division, and the mud clast abundance and size within, is highly variable over short length-scales. A-B) Bed character at log sites 1 through to 4. C-D) Mud-clast-rich sandstone near log position 1. E) Low angle stratification and unstratified sandstone near the base of bed at log position 2.

Fig. 13. Sole structures record flow deflection commencing between Locations V and IV during early deposition of the study interval (Package A) whilst during later deposition of the study interval (Package B) the zone of flow deflection is inferred to have advanced north beyond Location I. Such shift in the zone of deflection is resultant of basin floor aggradation within a basin with inclined basin margins (*sensu* Kneller and McCaffrey, 1999) and does not record a change to an unconfined setting as bed thicknesses remains similar (Fig. 1d) and current ripple lamination records continued reflection of flow away from the northern basin margin (Fig. 1d).

Fig. 14. Discounted mechanisms for the development of sandstone deposits containing a distinct mud-clast-rich division within the Costa Grande Member study interval. (A) Sandstone bed amalgamation between successive gravity currents *sensu* Walker (1966). (B) Substrate deformation and sandstone bed amalgamation beneath high concentration (modified from Butler and Tavarnelli (2006). (C) Gravity current triggered destabilisation of muddy slopes on confining sea floor topography (*sensu* Kneller and McCaffrey, 1999).

Fig. 15. Contrasting flow dynamics and depositional trends between confined and contained (CC) settings and confined uncontained (CU) settings. The interaction of gravity flow with multiple surrounding basin margins in CC settings results in a confined flow with extensive and complex three dimensional flow dynamics; such flow characteristics contribute to the prevention of developing localised depositional trends adjacent to confining topographic features and the prevention of developing systematic depositional trends on a basin scale. Gravity flow interaction with fewer confining topographic features in CU settings is thought to result in relatively localised confined flow with simpler three dimensional flow dynamics which favours the development of localised depositional trends adjacent to confining topography as documented by others in CU settings (e.g., Barker et al., 2008, Patacci et al., 2014).

Figure 1

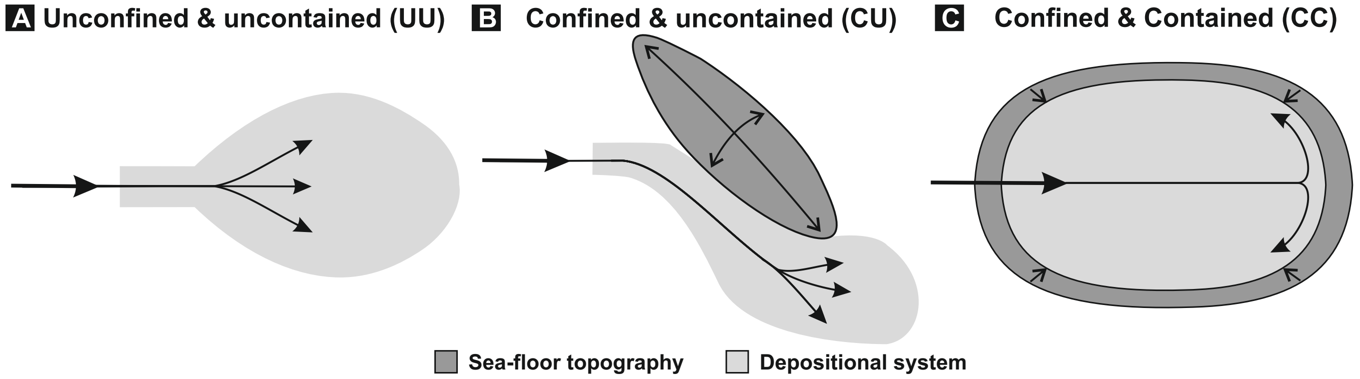
A Unconfined & uncontained (UU)
B Confined & uncontained (CU)
C Confined & Contained (CC)
Sea-floor topography
Depositional system

Figure 2

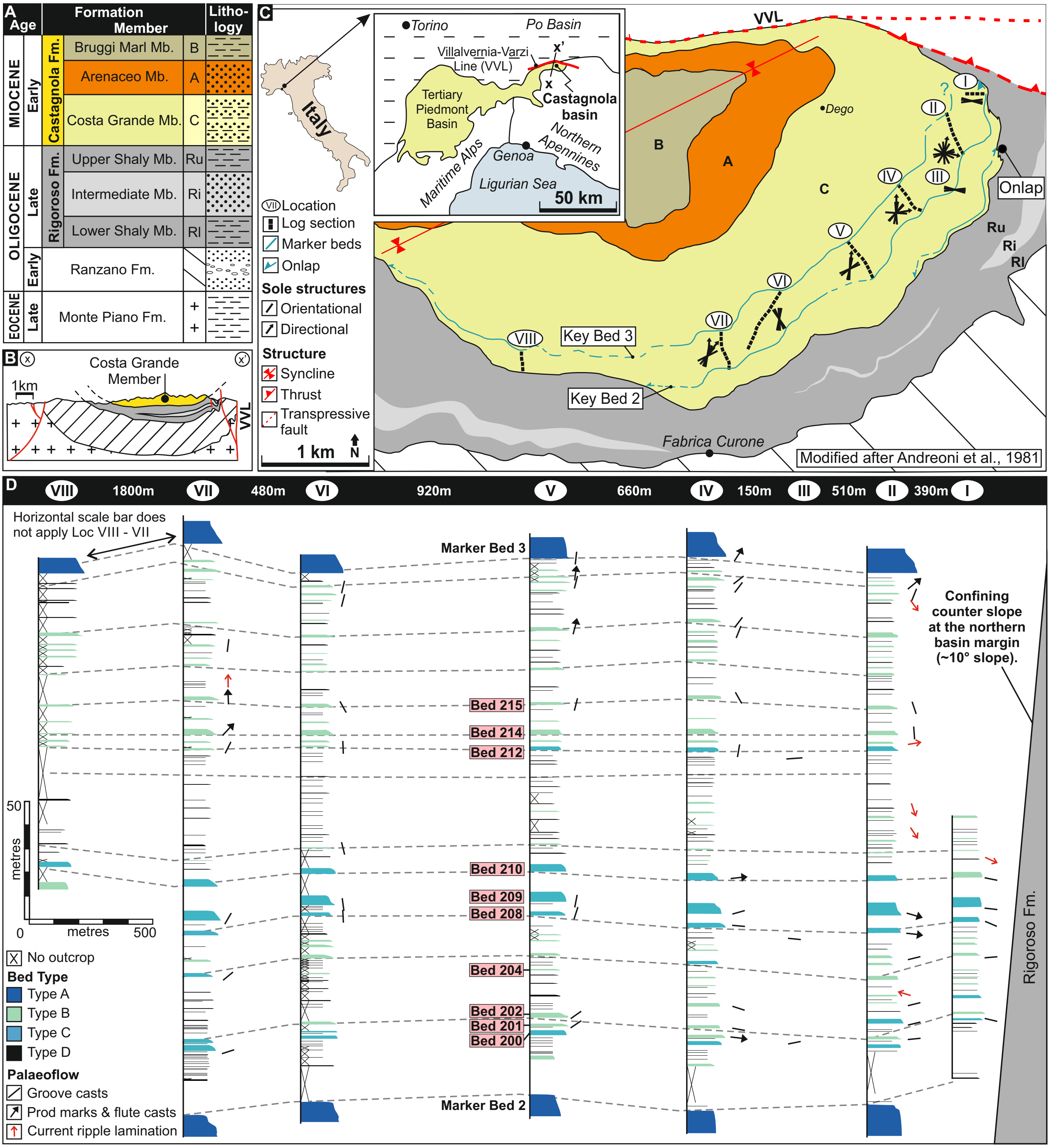

A
Age
Formation Member
Litho-logy
MIOCENE
Early
Castagnola Fm.
Bruggi Marl Mb.
B
Arenaceo Mb.
A
Costa Grande Mb.
C
OLIGOCENE
Late
Rigoroso Fm.
Upper Shaly Mb.
Ru
Intermediate Mb.
Ri
Lower Shaly Mb.
Rl
Early
Ranzano Fm.
EOCENE
Late
Monte Piano Fm.
B
Costa Grande Member
1km
VVL
C
Italy
Torino
Po Basin
Villalvernia-Varzi Line (VVL)
Tertiary Piedmont Basin
Castagnola basin
Northern Apennines
Maritime Alps
Genoa
Ligurian Sea
50 km
Location
Log section
Marker beds
Onlap
Sole structures
Orientational
Directional
Structure
Syncline
Thrust
Transpressive fault
1 km
N
VVL
Dego
Onlap
Ru
Ri
Rl
Key Bed 3
Key Bed 2
Fabrica Curone
Modified after Andreoni et al., 1981
D
VIII
1800m
VII
480m
VI
920m
V
660m
IV
150m
III
510m
II
390m
I
Horizontal scale bar does not apply Loc VIII - VII
Marker Bed 3
Bed 215
Bed 214
Bed 212
Bed 210
Bed 209
Bed 208
Bed 204
Bed 202
Bed 201
Bed 200
Marker Bed 2
Confining counter slope at the northern basin margin (~10° slope).
Rigoroso Fm.
50
metres
0
metres
500
No outcrop
Bed Type
Type A
Type B
Type C
Type D
Palaeoflow
Groove casts
Prod marks & flute casts
Current ripple lamination

Figure 3

Type A

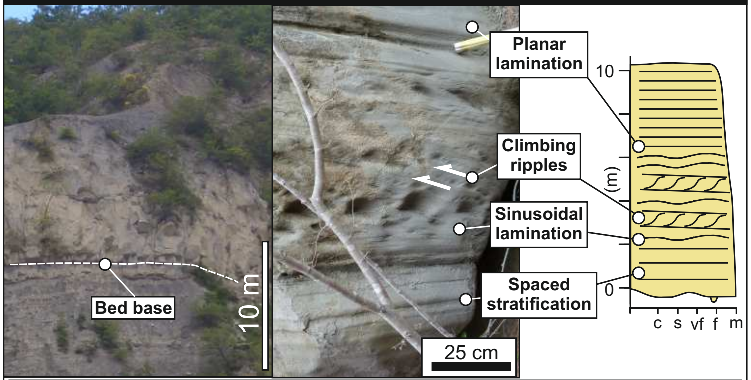

Key Characteristics	
Grain size	Fine to coarse sand
Thickness	Very thick beds (900 - 1300 cm)

- Alternations of unstratified and various laminated sand facies (e.g., planar, sinusoid, climbing ripple and current ripple lamination) in varying sequences.
- Thin basal traction carpets sometimes present (e.g., S2 of Lowe [1982] sequence).
- Current ripple lamination in opposing directions.
- Inverse & normal grain size grading.

Interpretation

- High sediment concentration flow (e.g., high density turbidity current *sensu* Lowe [1982]).
- Large volume / duration event.
- High suspension fall out rates (e.g., climbing & sinusoidal ripples).
- Flow interaction with, and reflection from the basin margin.

Type B

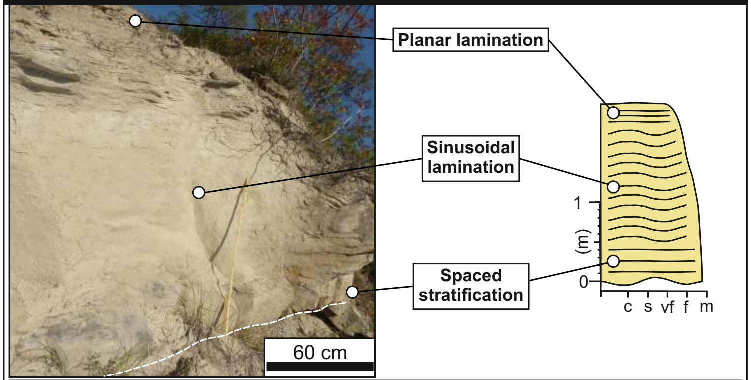

Key Characteristics	
Grain size	Fine to medium sand
Thickness	Thick to very thick beds (50 - 400 cm)

- Basal unstratified or crude laminated (wide spaced, 1 cm) sand overlain by variably laminated sand (e.g., sinusoidal, current ripple & planar lamination) in variable or repeating sequences.
- Erosive and non-erosive bases with partial entrainment of large muddy substrate clasts.
- Complex palaeoflow within individual beds.

Interpretation

- Erosive & high sediment concentration flow (e.g., high density turbidity current *sensu* Lowe [1982]).
- High suspension fall out rates (e.g., climbing & sinusoidal ripples).
- Flow interaction with, and reflection from the basin margin.

Type C

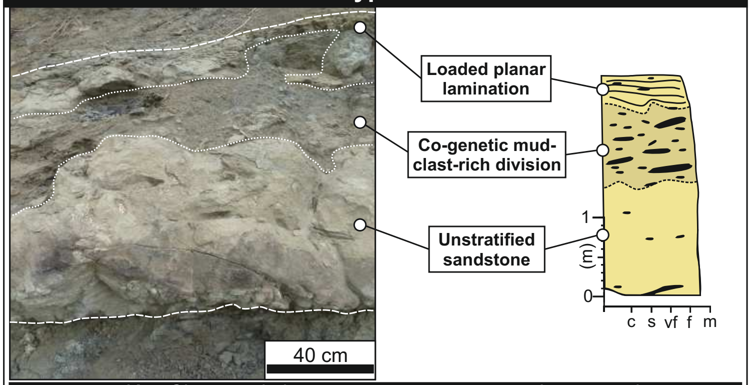

Key Characteristics	
Grain size	Fine to medium sand
Thickness	Thick to very thick beds (50 - 400 cm)

- Basal crudely laminated and / or unstratified sand overlain by a variable mud-clast-rich interval (sub-types C1, C2 & C3) followed by laminated sandstone.
- Mud-clast-rich interval thickness is highly variable on short (10 m) and long (1000 m) length-scales.
- Erosive bases common with evidence of entrainment of large (> 1 m) pieces of muddy substrate.
- Complex palaeoflow within individual beds.

Interpretation

- Erosive high sediment concentration flow (e.g., high density turbidity current *sensu* Lowe [1982]).
- Mud-clast populations reflect complexly distributed erosion.
- Flow interaction with, and reflection from the basin margin.

Type D

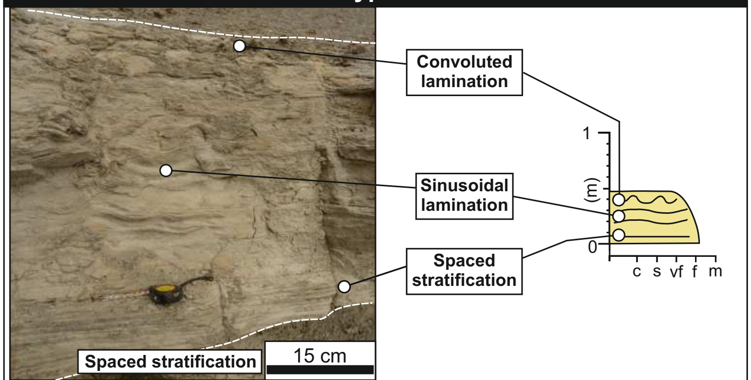

Key Characteristics	
Grain size	Silt to fine sand
Thickness	Very thin to thick beds(1 - 50 cm)

- Stratified beds typically commencing with spaced stratified sand overlain by varied arrangements of sinusoidal, climbing ripple, current ripple lamination.
- Examples of beds containing unstratified, slightly coarser grained, loaded sandstone sandwiched between underlying and overlying laminated sandstone.
- Mud-clast poor and non-erosive bases.
- Disperse current ripple lamination directions.

Interpretation

- Lower sediment concentration flow compared to those of bed types A-B (e.g., low density turbidity current *sensu* Bouma [1962]).
- High suspension fall out rates (e.g., sinusoidal ripples).
- Flow interaction with, and reflection from the basin margin.

Figure 4

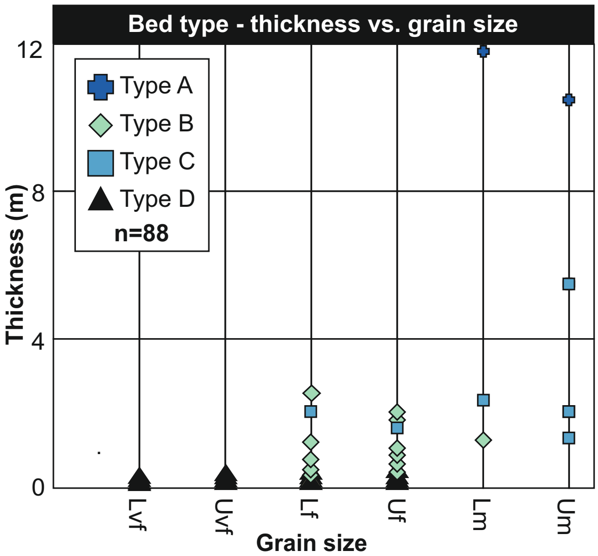
Bed type - thickness vs. grain size
Type A
Type B
Type C
Type D
n=88
Thickness (m)
12
8
4
0
Lvf
Uvf
Lf
Uf
Lm
Um
Grain size

Figure 5

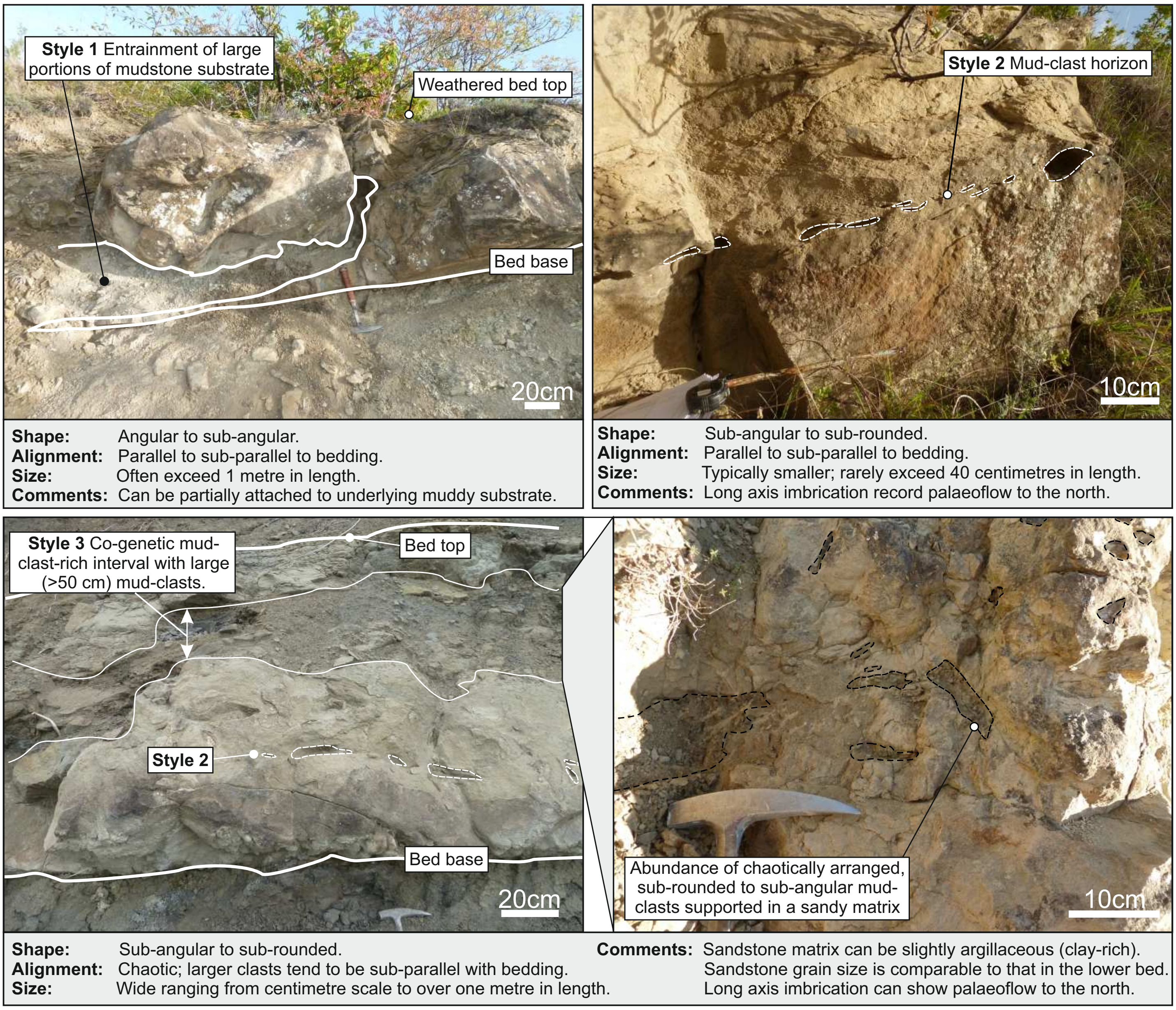
Style 1 Entrainment of large portions of mudstone substrate.
Weathered bed top
Bed base
20cm
Style 2 Mud-clast horizon
10cm
Shape: Angular to sub-angular.
Alignment: Parallel to sub-parallel to bedding.
Size: Often exceed 1 metre in length.
Comments: Can be partially attached to underlying muddy substrate.
Shape: Sub-angular to sub-rounded.
Alignment: Parallel to sub-parallel to bedding.
Size: Typically smaller; rarely exceed 40 centimetres in length.
Comments: Long axis imbrication record palaeoflow to the north.
Style 3 Co-genetic mud-clast-rich interval with large (>50 cm) mud-clasts.
Bed top
Style 2
Bed base
20cm
Abundance of chaotically arranged, sub-rounded to sub-angular mud-clasts supported in a sandy matrix
10cm
Shape: Sub-angular to sub-rounded.
Alignment: Chaotic; larger clasts tend to be sub-parallel with bedding.
Size: Wide ranging from centimetre scale to over one metre in length.
Comments: Sandstone matrix can be slightly argillaceous (clay-rich). Sandstone grain size is comparable to that in the lower bed. Long axis imbrication can show palaeoflow to the north.

Figure 6

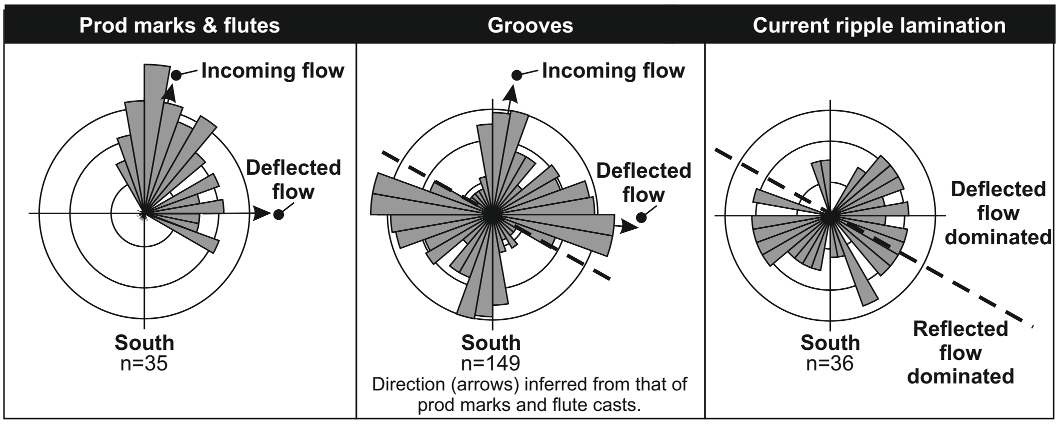

Prod marks & flutes
Grooves
Current ripple lamination
Incoming flow
Deflected flow
South
n=35
Incoming flow
Deflected flow
South
n=149
Direction (arrows) inferred from that of prod marks and flute casts.
Deflected flow dominated
Reflected flow dominated
South
n=36

Figure 7

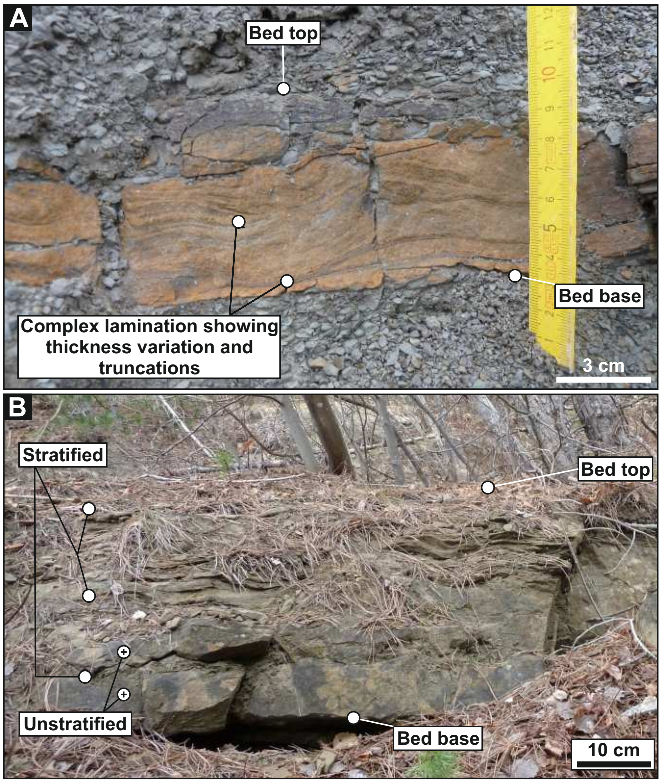

A
Bed top
Complex lamination showing thickness variation and truncations
Bed base
3 cm
B
Stratified
Bed top
Unstratified
Bed base
10 cm

Figure 8

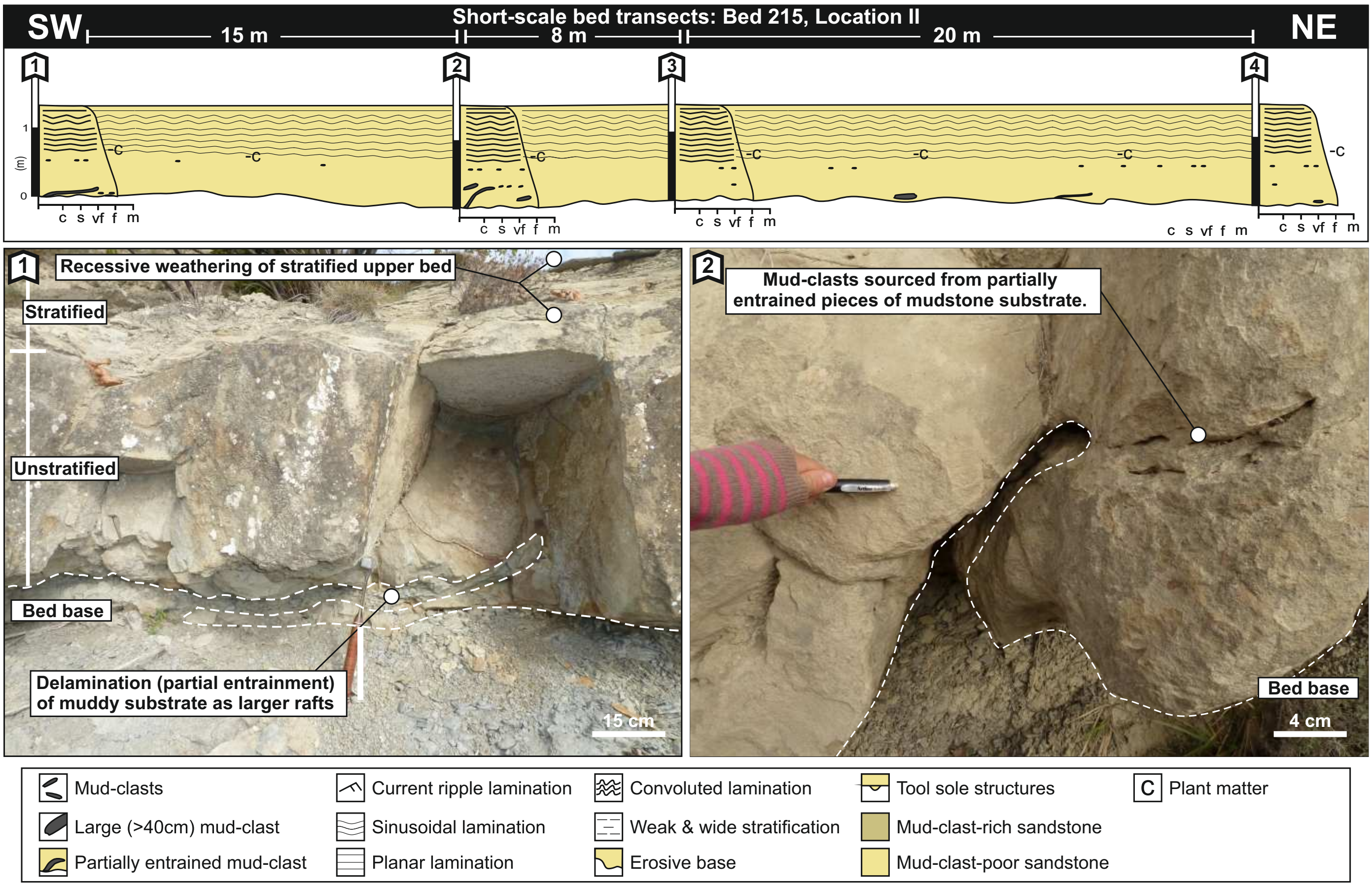

SW
NE
Short-scale bed transects: Bed 215, Location II
15 m
8 m
20 m
1
2
3
4
(m)
c s vf f m
Recessive weathering of stratified upper bed
Stratified
Unstratified
Bed base
Delamination (partial entrainment) of muddy substrate as larger rafts
15 cm
Mud-clasts sourced from partially entrained pieces of mudstone substrate.
4 cm
Mud-clasts
Large (>40cm) mud-clast
Partially entrained mud-clast
Current ripple lamination
Sinusoidal lamination
Planar lamination
Convoluted lamination
Weak & wide stratification
Erosive base
Tool sole structures
Mud-clast-rich sandstone
Mud-clast-poor sandstone
Plant matter

Figure 9

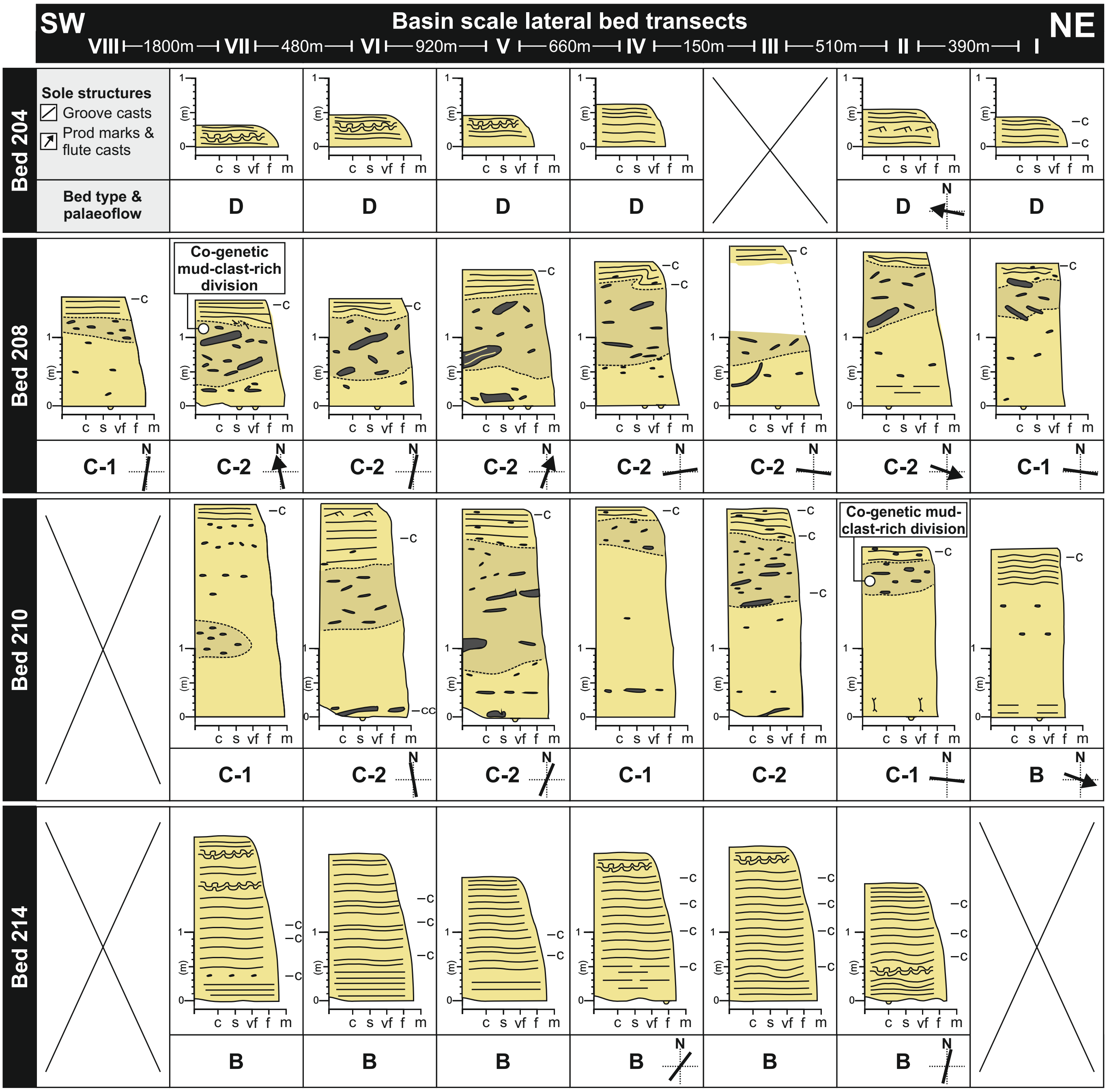
SW
Basin scale lateral bed transects
NE
VIII 1800m VII 480m VI 920m V 660m IV 150m III 510m II 390m I
Bed 204
Sole structures
Groove casts
Prod marks & flute casts
Bed type & palaeoflow
D
Bed 208
Co-genetic mud-clast-rich division
C-1
C-2
Bed 210
Co-genetic mud-clast-rich division
C-1
C-2
B
Bed 214
B
c s vf f m
(m)
N

Figure 10

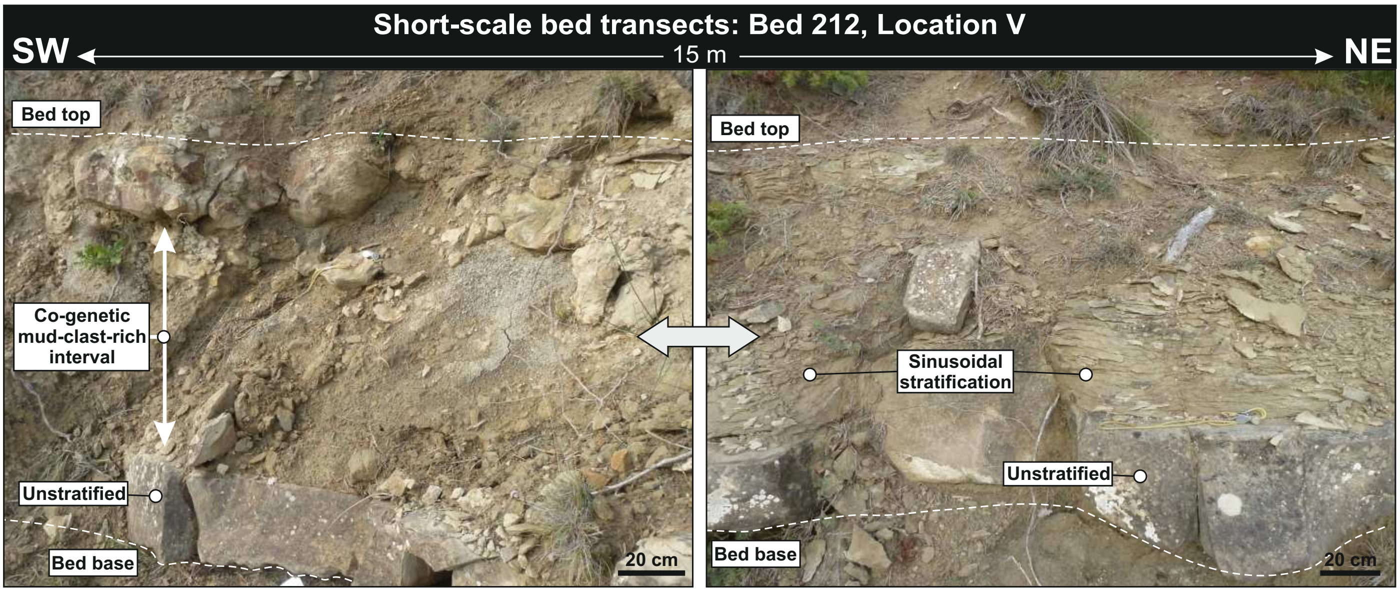
Short-scale bed transects: Bed 212, Location V
SW
15 m
NE
Bed top
Co-genetic mud-clast-rich interval
Unstratified
Bed base
20 cm
Bed top
Sinusoidal stratification
Unstratified
Bed base
20 cm

Figure 11

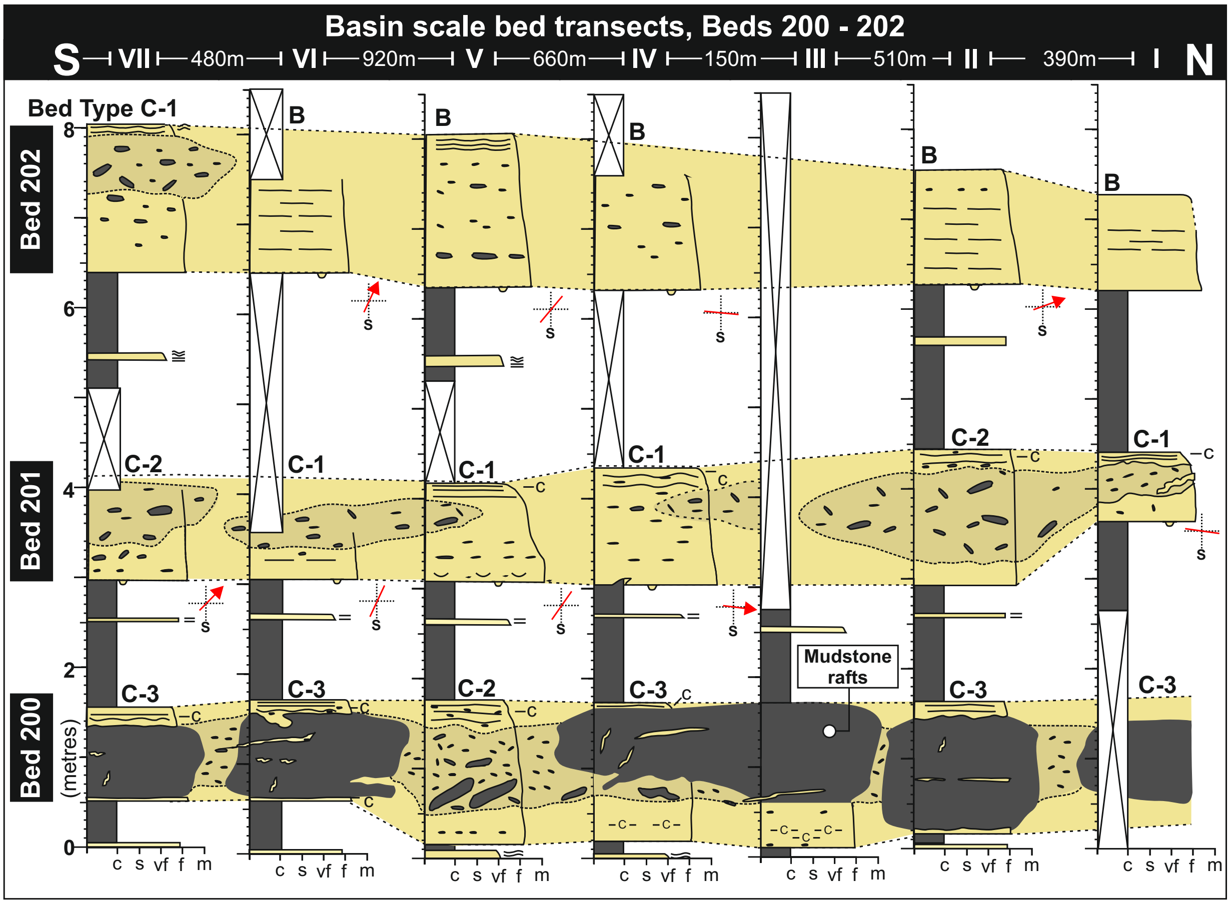

Basin scale bed transects, Beds 200 - 202
S VII 480m VI 920m V 660m IV 150m III 510m II 390m I N
Bed Type C-1
Bed 202
Bed 201
Bed 200
(metres)
B
C-1
C-2
C-3
Mudstone rafts
c s vf f m

Figure 12

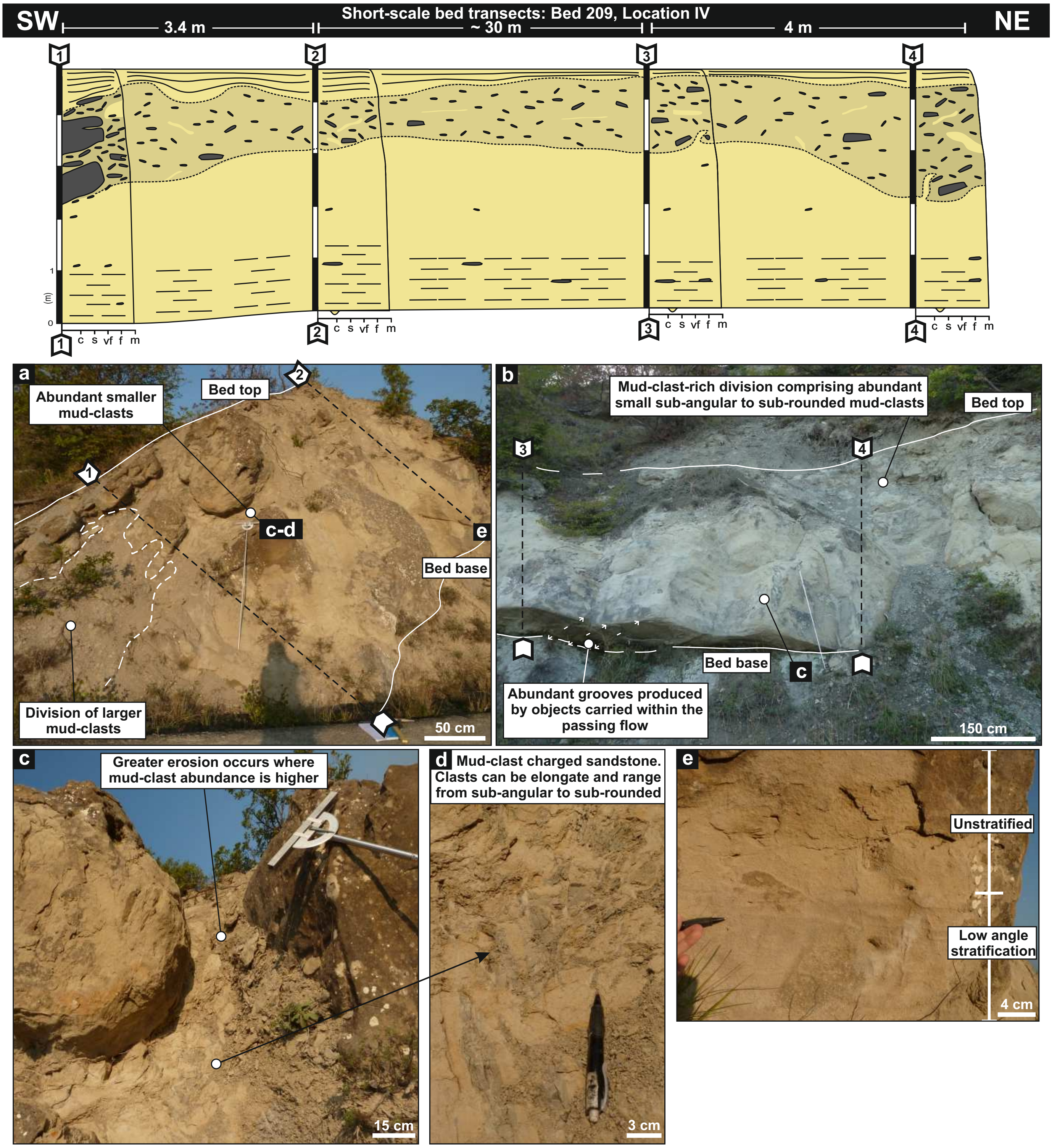

SW
Short-scale bed transects: Bed 209, Location IV
3.4 m
~ 30 m
4 m
NE
1
2
3
4
(m)
0
1
c s vf f m
a
Abundant smaller mud-clasts
Bed top
c-d
e
Bed base
Division of larger mud-clasts
50 cm
b
Mud-clast-rich division comprising abundant small sub-angular to sub-rounded mud-clasts
Bed top
Bed base
c
Abundant grooves produced by objects carried within the passing flow
150 cm
c
Greater erosion occurs where mud-clast abundance is higher
15 cm
d
Mud-clast charged sandstone. Clasts can be elongate and range from sub-angular to sub-rounded
3 cm
e
Unstratified
Low angle stratification
4 cm

Figure 13

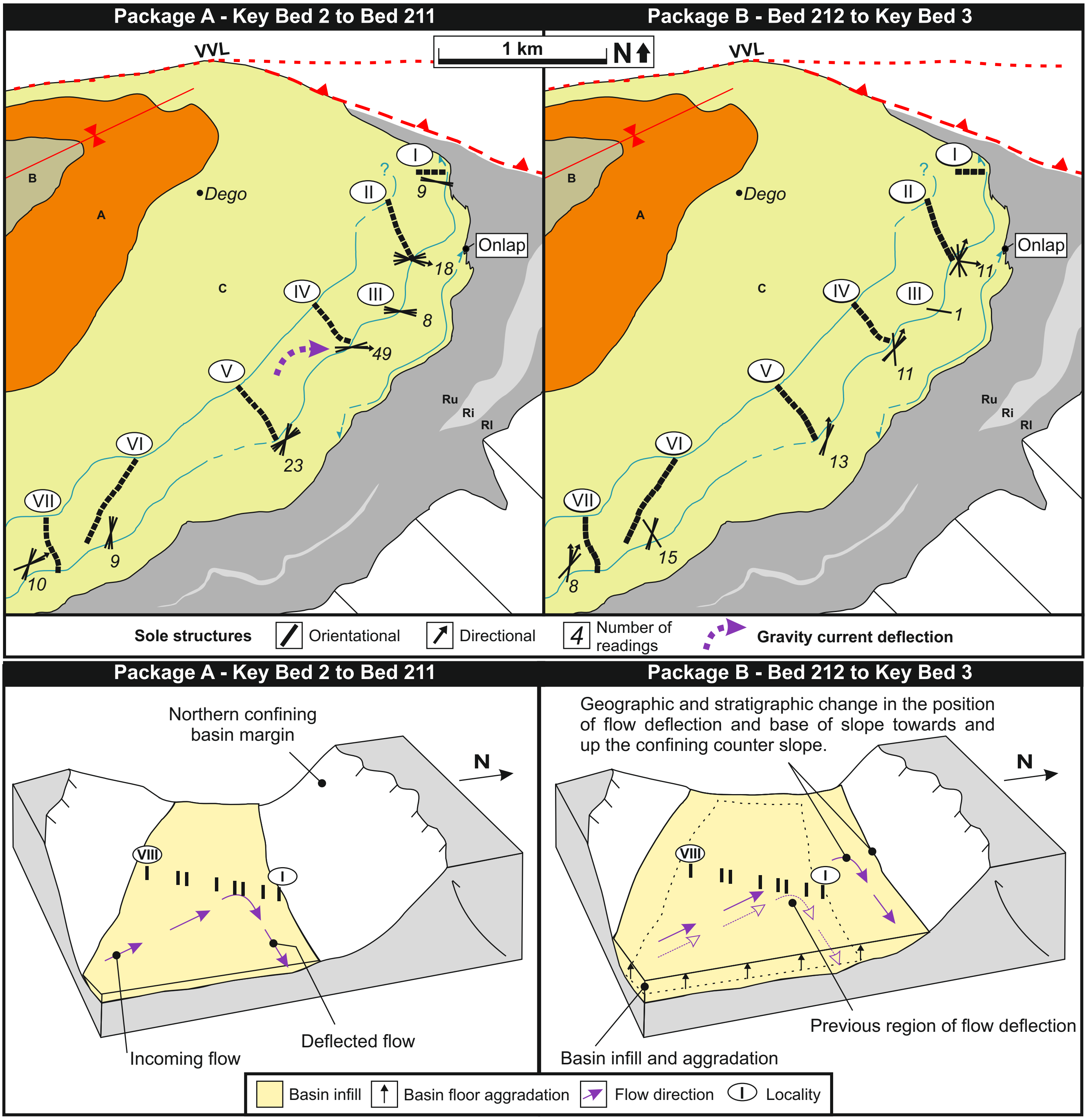
Package A - Key Bed 2 to Bed 211
Package B - Bed 212 to Key Bed 3
1 km
N
VVL
Dego
A
B
C
Onlap
Ru
Ri
Rl
I
II
III
IV
V
VI
VII
9
18
8
49
23
9
10
11
1
11
13
15
8
Sole structures
Orientational
Directional
4 Number of readings
Gravity current deflection
Package A - Key Bed 2 to Bed 211
Package B - Bed 212 to Key Bed 3
Northern confining basin margin
N
VIII
Incoming flow
Deflected flow
Geographic and stratigraphic change in the position of flow deflection and base of slope towards and up the confining counter slope.
Previous region of flow deflection
Basin infill and aggradation
Basin infill
Basin floor aggradation
Flow direction
Locality

Figure 14

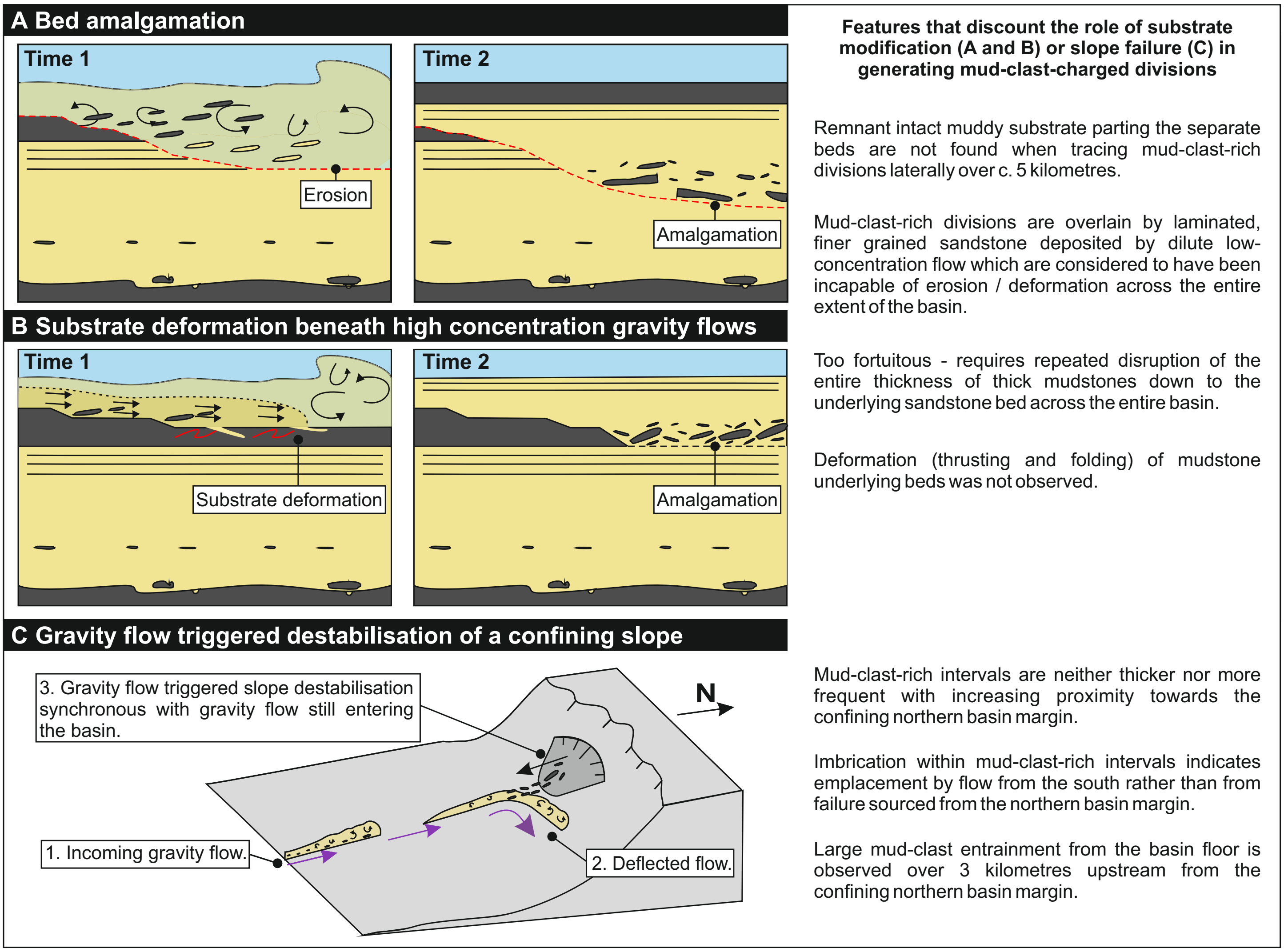

A Bed amalgamation
Time 1
Erosion
Time 2
Amalgamation
B Substrate deformation beneath high concentration gravity flows
Time 1
Substrate deformation
Time 2
Amalgamation
C Gravity flow triggered destabilisation of a confining slope
3. Gravity flow triggered slope destabilisation synchronous with gravity flow still entering the basin.
N
1. Incoming gravity flow.
2. Deflected flow.
Features that discount the role of substrate modification (A and B) or slope failure (C) in generating mud-clast-charged divisions
Remnant intact muddy substrate parting the separate beds are not found when tracing mud-clast-rich divisions laterally over c. 5 kilometres.
Mud-clast-rich divisions are overlain by laminated, finer grained sandstone deposited by dilute low-concentration flow which are considered to have been incapable of erosion / deformation across the entire extent of the basin.
Too fortuitous - requires repeated disruption of the entire thickness of thick mudstones down to the underlying sandstone bed across the entire basin.
Deformation (thrusting and folding) of mudstone underlying beds was not observed.
Mud-clast-rich intervals are neither thicker nor more frequent with increasing proximity towards the confining northern basin margin.
Imbrication within mud-clast-rich intervals indicates emplacement by flow from the south rather than from failure sourced from the northern basin margin.
Large mud-clast entrainment from the basin floor is observed over 3 kilometres upstream from the confining northern basin margin.

Figure 15

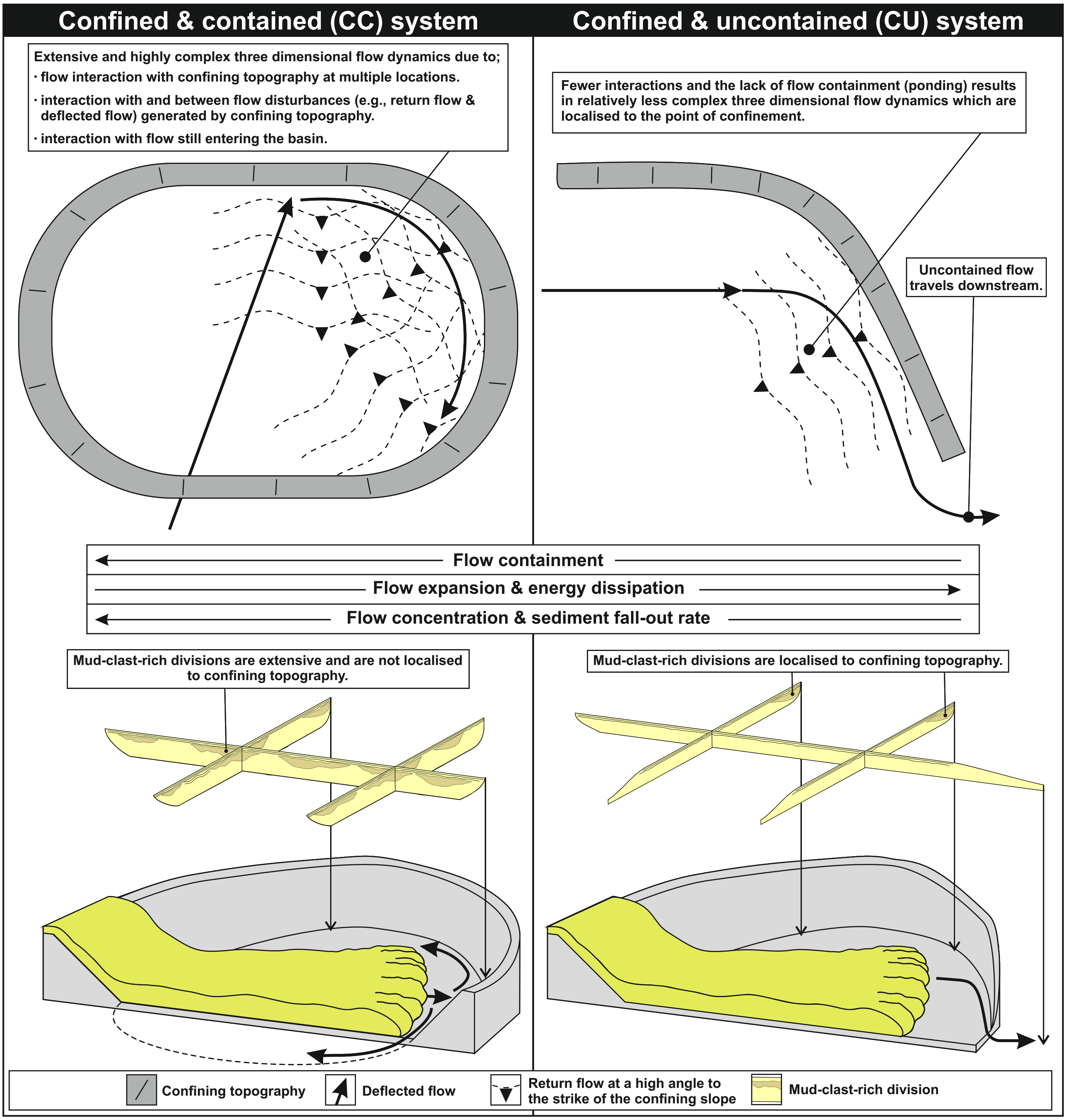

Confined & contained (CC) system
Confined & uncontained (CU) system
Extensive and highly complex three dimensional flow dynamics due to;
· flow interaction with confining topography at multiple locations.
· interaction with and between flow disturbances (e.g., return flow & deflected flow) generated by confining topography.
· interaction with flow still entering the basin.
Fewer interactions and the lack of flow containment (ponding) results in relatively less complex three dimensional flow dynamics which are localised to the point of confinement.
Uncontained flow travels downstream.
Flow containment
Flow expansion & energy dissipation
Flow concentration & sediment fall-out rate
Mud-clast-rich divisions are extensive and are not localised to confining topography.
Mud-clast-rich divisions are localised to confining topography.
Confining topography
Deflected flow
Return flow at a high angle to the strike of the confining slope
Mud-clast-rich division